2019-12-13

Contrasts in Oxygen Variability of SE Pacific Oxygen Deficient Zone and Subtropical Gyre

Molly M. Martin
University of Miami, mmmartin@rsmas.miami.edu

UNIVERSITY OF MIAMI

CONTRASTS IN OXYGEN VARIABILITY OF SE PACIFIC OXYGEN DEFICIENT ZONE AND SUBTROPICAL GYRE

By

Molly M. Martin

A THESIS

Submitted to the Faculty
of the University of Miami
in partial fulfillment of the requirements for
the degree of Master of Science

Coral Gables, Florida

December 2019

UNIVERSITY OF MIAMI

A thesis submitted in partial fulfillment of
the requirements for the degree of
Master of Science

CONTRASTS IN OXYGEN VARIABILITY OF SE PACIFIC OXYGEN DEFICIENT ZONE AND SUBTROPICAL GYRE

Molly M. Martin

Approved:

_____ Rana A. Fine, Ph.D. Professor of Ocean Sciences	_____ Dennis A. Hansell, Ph.D. Professor of Ocean Sciences
_____ Victoria Coles, Ph.D. Associate Professor University of Maryland	_____ Guillermo Prado, Ph.D. Dean of the Graduate School

MARTIN, MOLLY M. (M.S., Ocean Sciences)
Contrasts in Oxygen Variability of SE Pacific Oxygen Deficient Zone and Subtropical Gyre (December 2019)

Abstract of a thesis at the University of Miami.

Thesis supervised by Professor Rana Fine.
No. of pages in text. (57)

Two decades of observations in the eastern South Pacific show changes in oxygen concentrations and apparent oxygen utilizations (AOUs) in the lower thermocline 26.5-27.0 σ_θ. The 2013 GEOTRACES O_2 and AOU data along ~12°S from the oxygen deficient zone (ODZ; O_2 < 50 μmol/kg) are compared with repeat hydrography data from the 1990s to the 2010s; the recent data add detail and process information to earlier work. In 2013, transient tracer ratio ages suggest renewal times of over two decades at the core of the ODZ as compared with being at least 7 years younger at the same densities in the subtropical gyre. Related to the age differences in the two regions, we observe oxygen parameters changing in different directions over the two decades, also different processes and forcing dominate. Similar to earlier studies, we found subtropical gyre oxygen concentrations increase and AOUs decrease due to increases in ventilation between 1990s and 2013, coupled to changes in southern hemisphere westerlies. In the core of the ODZ, oxygen concentrations decrease at an annual rate of 0.2 μmol/kg/yr, AOUs increase between 1990s and 2013, and the 5 μmol/kg contour reaches ~300 m deeper in the water column. ODZ changes are estimated to be due to increased biological consumption, consistent with increased upwelling corresponding to increased trade winds during that period. Thus, the difference in oxygen between the 1990s and 2013 is due to - proximity

of the ODZ to coastal upwelling and longer ventilation time scales in the ODZ than gyre. In the gyre, water masses are closer to their sources and ages are younger. Whereas, the ODZ is more isolated from water mass source regions, and it takes more than two decades for the ventilated gyre waters to reach the ODZ. We have shown that in the South Pacific changes in oxygen parameters in the ODZ and subtropical gyre – to date – appear to be due to independent processes and forcing acting in each region. Continuing ocean observations are needed to monitor changes in gases such as oxygen that are critical to life.

TABLE OF CONTENTS

LIST OF FIGURES

LIST OF TABLES

Chapter 1: **Introduction**

Increased warming and stratification due to climate change are predicted to affect ventilation of the ocean with gases such as oxygen (e.g., Capotondi et al., 2012; Keeling et al., 2010) and increase microbial biological consumption of oxygen (Brewer and Peltzer, 2017). Indeed, studies of changes in oxygen show a global decline for at least two decades, which is not dominated by saturation changes (e.g., Ito et al., 2017). The oxygen decline is not uniform across the ocean, and one of the regions where oxygen has been shown to decrease is in tropical oxygen deficient zones (ODZs) (e.g., Stramma et al., 2010, 2008). Large-scale ODZs are observed at the tropical and eastern parts of the Pacific and Atlantic subtropical gyres. The ODZs are low in oxygen, and will be defined as less than 50 μmol/kg in this study. Also, the ODZs are largely bypassed by the oxygen rich subtropical gyre circulations (Luyten et al., 1983), and are adjacent to coastal regions with high productivity (e.g., Blanchette et al., 2009). A cruise in 2013, the GEOTRACES Eastern Pacific Zonal Transect (EPZT) along ~12ºS from the coast of Peru through the ODZ to 150ºW in the equatorward part of the subtropical gyre, provides data to compare to hydrographic data from the 1990s through the 2010s. The South Pacific subtropical gyre is the largest subtropical gyre in size and the most oligotrophic. Although changes in oxygen parameters have been documented in the South Pacific, we are adding new detail and adding to an understanding of the processes causing the changes. Our objective is to analyze changes in oxygen parameters and examine the underlying causes along ~12ºS from the ODZ into the equatorward part of the subtropical gyre and examine connections between the two circulation regions. Specifically, we compare oxygen concentrations and apparent oxygen utilizations (AOUs), and estimate oxygen utilization rates (OURs), over

two decades along 12ºS and in the lower thermocline layer 26.5-27.0 σ_θ. The layer is at the core of the ODZ. The layer encompasses tropical waters and the large volume, well ventilated Subantarctic Mode Water (SAMW); some remnant of SAMW mixing products are transported to the ODZ (e.g., Fine et al., 2001).

Earlier studies showed that the South Pacific subtropical gyre waters contribute to ventilation of the ODZ mostly via the eastward flowing tropical currents (e.g., Wyrtki, 1974; Lukas, 1986; Fine et al., 1987; Stramma et al., 2010; Czeschel et al., 2015; Llanillo et al., 2018). These studies describe the supply pathways of water to the ODZ from tropical eastward flowing currents: Equatorial Undercurrent, Southern Subsurface Countercurrent, and Southern Intermediate Countercurrent. Also transporting recently ventilated thermocline and intermediate water gyre water is the westward flowing South Equatorial Current, which forms the equatorward part of the subtropical gyre. On the eastern side of the gyre, the Peru (Humboldt) Current transports water northwards offshore of the upwelling region. A recently study by Llanillo et al. (2018) analyze oxygen advective and diffusive fluxes into the South Pacific ODZ to quantify oxygen contributions from subtropical versus tropical equatorial pathways. In their middle layer, the core of the ODZ that most closely coincides with our lower thermocline layer, they find tropical water contributions dominate over subtropical in a ratio of about 60:40. Recent observations also in 2013 by Sonnerup et al. (2019) show an increase in transient tracer depth penetration of ~250 m to 800 m in the coastal ODZ region 12-22ºS, 70-86ºW, as compared with an occupation two decades earlier. This result shows that water ventilated less than sixty years ago has reached the coastal waters of the ODZ, the Sonnerup study at 800 m is deeper and westward of our focus.

First, we briefly review earlier studies on variability in oxygen in the South Pacific ODZ and the equatorward part of the adjacent subtropical gyre. Then there is a description of data and the methods, results are presented and discussed, and conclusions are drawn.

1.1 *Oxygen Variability in the ODZ*

Previous studies of the South Pacific ODZ (Czeschel et al., 2015, 2012; Stramma et al., 2008) show its vertical expansion and a decrease in oxygen content over 30-50 years. Stramma et al. (2010) describe an eastward flux of oxygen in the zonal currents along with a decrease in oxygen content equatorward of the South Pacific ODZ over nearly 30 years (1990-2008). Schmidtko et al. (2017) use historical data to show a 1.3% decrease in oxygen content from 1960-2010. Their results apply to the equatorial Pacific from 15ºN to 15ºS from 0-1200 m; this region includes the equatorial current system as well as parts of the North and South Pacific ODZs. Duteil et al. (2014) point out that local changes in the trade winds could play a key role in oxygen variability. For example, a weakening (strengthening) in the trades should decrease (increase) the upwelling, biological activity and oxygen demand within the ODZ (as discussed for the eastern tropical North Pacific by Deutsch et al., 2014).

These earlier studies focused on changes in oxygen in the equatorial region of the Pacific, which is north of the main part of the South Pacific ODZ. We are concentrating on the region along and poleward of 12ºS where the ODZ is the strongest, i.e., lowest in oxygen. Furthermore, we will try to differentiate between physical and biological effects on oxygen parameters, which will take the work further than earlier studies.

1.2 ***Oxygen Variability in the Subtropical Gyre***

While several reasons for AOU changes have been discussed for the North Pacific subtropical gyre (e.g., Mecking et al., 2008), in the South Pacific decadal changes in the gyre circulation have been related to southern hemisphere winds (Roemmich et al., 2016, 2007). Roemmich et al. (2016) show a trend of increasing South Pacific gyre circulation, with an increase in southern hemisphere westerly winds starting in mid-1990s to 2014. Also, decadal changes in ventilation, particularly at the level of the SAMW, could have affected waters in the ODZ. Several studies using transient tracer data have shown an increase in South Pacific subtropical gyre ventilation in the decade between 1990s and 2000s (e.g., Fine, 2011; Waugh et al., 2013; Fine et al., 2017). In addition, Fine et al. (2017), looking at the density range of SAMW, showed a corresponding decrease in AOU, which they attributed to changes in the southern hemisphere winds. Thus, based on earlier studies, we expect to see changes in oxygen parameters along 12ºS between the 1990s and 2010s.

Chapter 2: **Data**

We use recent and historical oxygen, nutrient, transient tracer and hydrographic data. The recent GEOTRACES 2013 South Pacific cruise was from the coast of Peru to ~150°W along ~12°S, along the equatorward part of the subtropical gyre (Fig. 2.1 and 2.2). During this cruise 36 stations were sampled from the surface to ~5000 m. GEOTRACES data are compared to hydrographic data that cross 12°S from the 1990s, 2000s, and 2010s repeat hydrography cruises (WOCE, CLIVAR, and GO-SHIP; from P16 along 150°W, P17 along 135°W, P18 along 105°W, and P19 along 88°W). Additional hydrographic data and oxygen values were obtained from ARGO floats. The repeat hydrography cruises have 0.5º station spacing and GEOTRACES has ~2.5º spacing. For this reason, in order to compare the various data, the repeat hydrography cruises are averaged over 2-5º while GEOTRACES data are averaged over ~5º. Practically, at least 3 stations of data were averaged to diminish the effects of bias from fronts and eddies (radius of deformation along 12ºS is ~1º). CTD data for temperature, salinity, and oxygen are used for increased vertical resolution. Oxygen parameters from datasets of different years are compared using potential density rather than depth to limit the effects of water mass heave.

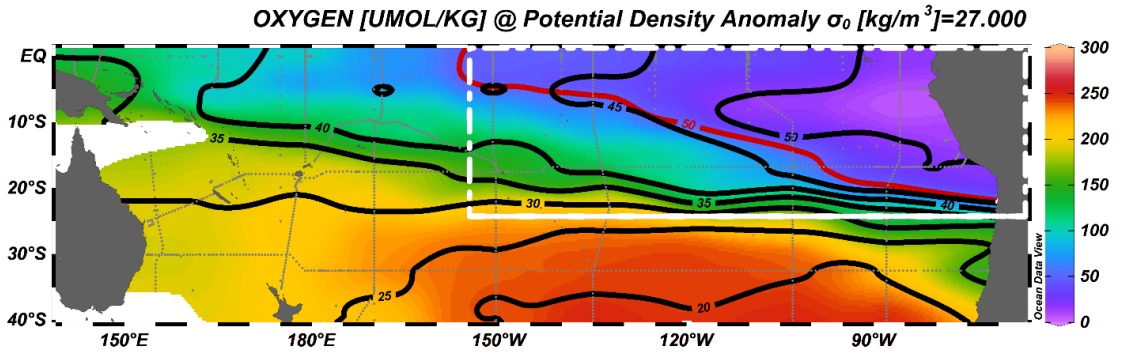

Figure 2.1. Map of bottle oxygen concentrations on 27 σ_θ from 1990s GLODAP dataset (Olsen et al., 2016). The color bar on right shows oxygen concentrations from 0 to 300 µmol/kg. The red contour shows the average location of the 50 µmol/kg oxygen contour. The grey dotted lines show the locations of historical stations. The black contours show the pCFC-12 age in years. The white box highlights the location of interest as shown in Figure 2.2.

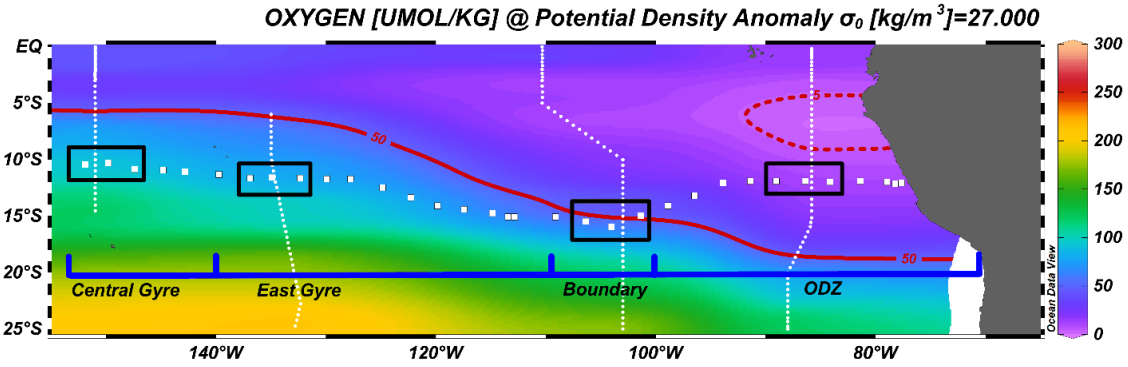

Figure 2.2. Map of CTD oxygen concentrations on 27 σ_θ from 1990s WOCE data. The color bar on right shows oxygen concentrations from 0 to 300 µmol/kg. The red contour depicts the average location of the 50 µmol/kg oxygen contour and the dotted red line depicts the average location of the 5 µmol/kg oxygen contour. The blue line shows our largescale division into ODZ, boundary and gyre regions. The white squares show the station locations of the GEOTRACES 2013 EPZT section. The black boxes show the stations from GEOTRACES that are compared to historical meridional stations along the white dotted lines. In the ODZ region, there are WOCE data from P19 (1993) between 11-13ºS. In the boundary region, there are P18 data from WOCE (1994) and CLIVAR (2007) between 13.5º-16.5ºS. In the east gyre region, there are P17 data from WOCE (1991) between 10.5º-12.5ºS. In the central gyre region, there are P16 data from WOCE (1991) and CLIVAR (2006) between 11.5-13.5ºS.

The GEOTRACES data were divided into three regions to focus on changes in oxygen parameters: ODZ, boundary, gyre (Fig. 1). On the westward extreme, the GEOTRACES cruise track from 110ºW to ~150ºW along ~12ºS was along the equatorward part of the South Pacific subtropical gyre. We divide the gyre into central and east to take advantage of locations of historical crossover stations. The east gyre in 2013 and the 1990s has average oxygen concentrations at or above 50 μmol/kg, and in central gyre concentrations are above 70 μmol/kg. On the eastward extreme, the ODZ is defined from the coast of Peru to 100ºW; this is where oxygen concentrations are below 50 μmol/kg in the layer of interest and a large portion has oxygen concentrations below 5 μmol/kg. The part of the ODZ we are focusing on is between 84°W and 89°W based upon availability of 1990s data to use for comparison. The 5 μmol/kg contour does not extent further westward than 100ºW. The ODZ is characterized as a region isolated by the gyre circulation; however, it has high productivity due to proximity to coastal upwelling.

The boundary region between the ODZ and subtropical gyre is defined as the area between 100ºW and 110ºW. By the nature of it being a boundary region, there is a substantial amount of temporal variability, though much of the boundary has oxygen concentrations below and approaching the 50 μmol/kg. There are large differences in temperature and salinity, suggesting the presence of different water masses in the region (Fig. 2.3). The northern as compared with the southern stations have higher salinity and are closer in T-S properties to those in the ODZ (Fig. 2.3, Table 1). As the northern stations are closer in properties to the ODZ, we refer to these stations as the northeast boundary region (Fig. 2.4). Similarly, the southern stations are closer in T-S properties to

the gyre, we refer to these stations as the southwest boundary region. Some of the cruises occurred during different times of the year and the seasonal changes in the location of the boundary between the ODZ and gyre make it difficult to base the division of northeast and southwest by location only, which is why T-S were used. In addition, only 1990s and 2010s data capture both boundary regions. The 2000s data is grouped in the northeast boundary region due to T-S similarities; other 2000s stations within the latitudes of the boundary region are not used due to the presence of eddies. Based on similar reasoning, GEOTRACES stations are grouped into the southwest boundary region based on T-S properties.

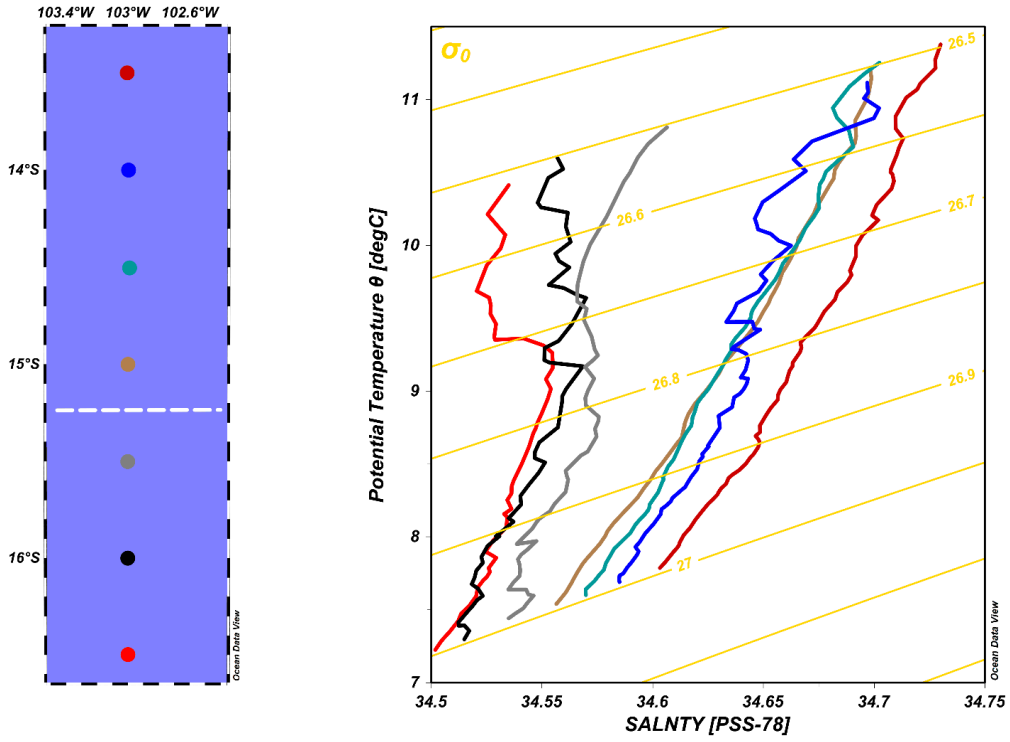

Figure 2.3. A CTD Temperature/Salinity plot of 1990s boundary stations showing the northeast (red, blue, green gold) and southwest (gray, black, pink) boundary regions. The map to the left shows station locations, and the dashed white line indicates the border of the two regions.

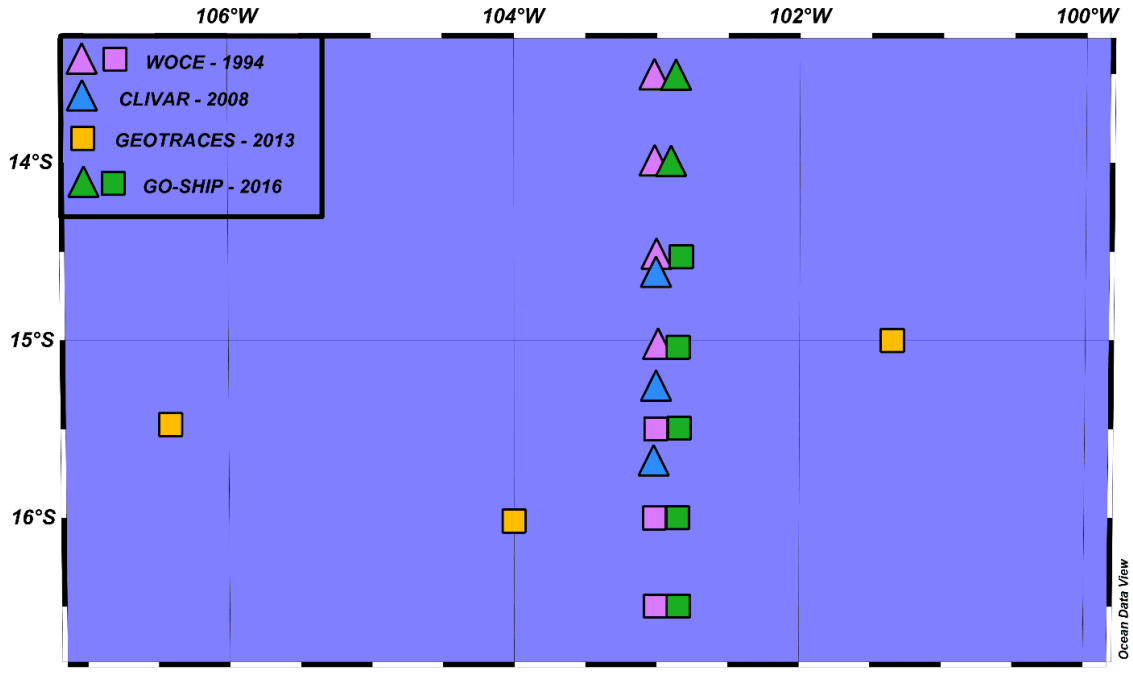

Figure 2.4. Map of boundary station locations. The triangles indicate stations used in the northeast boundary region, while the squares indicate stations used in the southwest boundary region.

The layer of interest is in the density range 26.5-27.0 σ_θ and was chosen for several reasons. It is the core of the ODZ - that is where oxygen concentrations are the lowest (vertical minimum in GEOTRACES dataset). The chlorofluorocarbons (CFCs) and sulfur hexafluoride (SF_6) are generally at measurable concentrations down to 27.0 σ_θ. The upper boundary of the chosen layer (26.5 σ_θ) is well below the mixed layer and it is where differences in oxygen concentrations between the two decades become significant. The density range 26.5-27.0 σ_θ is in the ~200-550 m depth range, and includes water from several sources. There are waters from the equatorial region as well as the large volume, well-ventilated SAMW, which is centered at approximately 26.8 σ_θ. By further dividing this density range into layers, examining details in the trends is facilitated. The

density range was divided into three layers: layer 1 (26.5-26.67 σ_θ), layer 2 (26.67-26.78 σ_θ), and layer 3 (26.78-27 σ_θ). The layers were chosen to be similar to the densities used by Llanillo et al. (2018) when converted from neutral density to potential density.

Chapter 3: **Methods**

This section describes the methods used as follows: water mass ages for estimating ventilation timescales, oxygen utilization rates (OURs), O_2^* for differentiating between biological and physical processes in the changes in oxygen parameters, and potential vorticity for examining changes in stratification. In addition, errors are estimated for the measured and derived terms.

3.1 ***Water Mass Ages***

The transient tracers - CFC-11, CFC-12 and SF_6 - are used to estimate water mass ages and oxygen utilization rates. Here, tracer ages are calculated using the ratios of two partial pressures. The partial pressure for each transient tracer is calculated using the seawater concentration (C) and the solubility function (F), potential temperature (θ) and salinity (S) (e.g., Doney and Bullister, 1992):

$$pCFC = C/F(\theta, S)$$

Laboratory measurements for solubility (F) were made by Warner and Weiss (1985) for CFC-11 and CFC-12 and Wanninkhof et al. (1991) and Bullister et al. (2002) for SF_6. The tracer age is estimated by comparing the partial pressure to the atmospheric time history (Fig. 3.1). For recent datasets, when SF_6 has been measured (since ~2008); the pSF_6/pCFC-11 or pSF_6/pCFC-12 ratio is used.

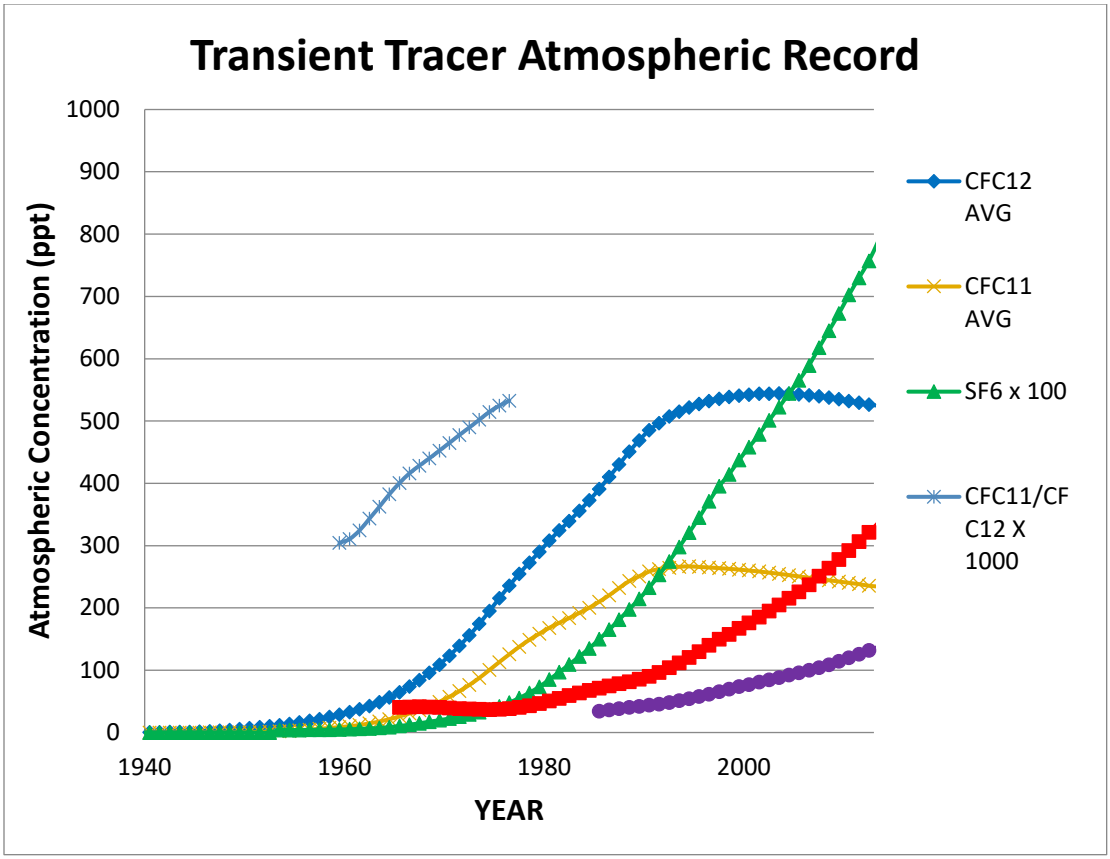

Figure 3.1. Atmospheric history of CFC-11, CFC-12, CFC-11/CFC-12, SF_6/CFC-11, SF_6-/CFC-12 and SF_6 concentrations (parts per trillion - ppt) (Bullister, 2015). SF_6 is multiplied by 100, CFC-11/CFC-12 is multiplied by 1000 and plotted for the years that the ratio is linear in the atmosphere, and SF_6/CFC-11 is multiplied by 10000.

There is good agreement between the pSF_6/pCFC-11 and pSF_6/pCFC-12 ratio ages from the 2013 data (Fig. 3.2), with a 0.9 correlation. Also, there is an offset of ~1.4 years, with the pSF_6/pCFC12 ages being slightly older on average. For 2000s and 2010s (CLIVAR and GO-SHIP), pSF_6/pCFC11 ratio is used as it has a larger dynamic range than pSF_6/pCFC12. For GEOTRACES (2013) data the pSF_6/pCFC12 ratio is used since there are more CFC12 data than CFC11 that exceed the minimum concentration criteria (see below). The pCFC-11/pCFC-12 ratio is used for the 1990s data as there were no SF_6. This ratio can be used for waters older than 1976, since the ratio reached a maximum

afterwards (Fig. 3.1). A benefit of the ratio age over a single partial pressure age is that the surface saturation does not need to be estimated. For this reason and to lessen the effects of mixing, we are using ratio ages.

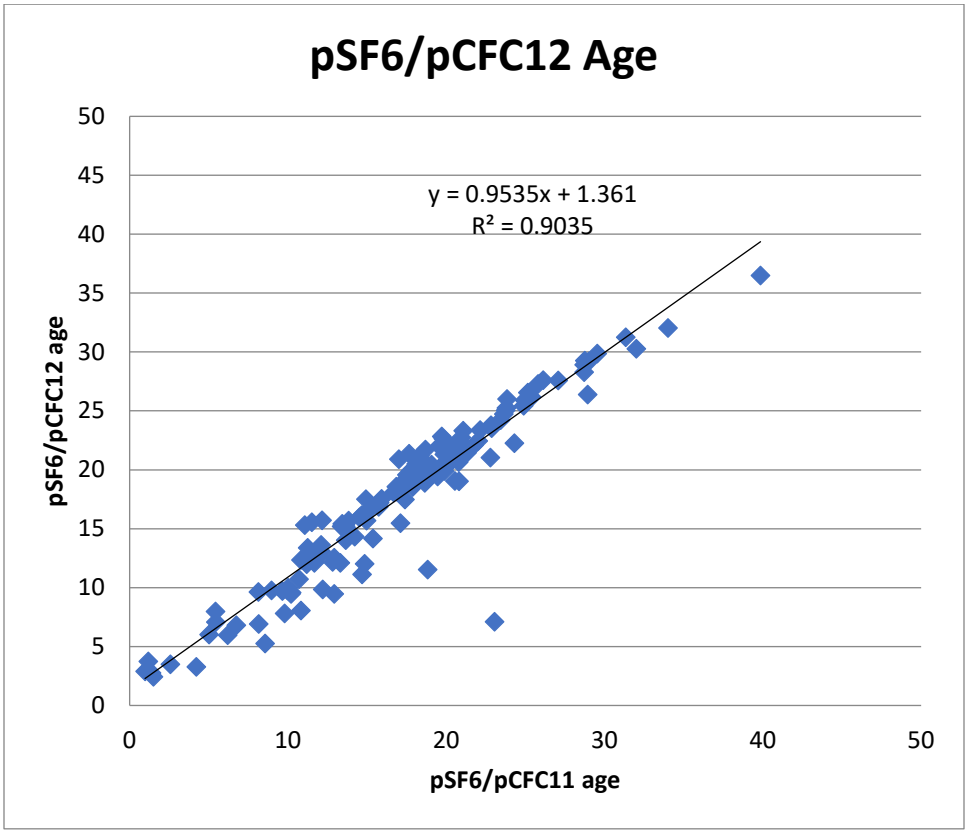

Figure 3.2. Plot of the GEOTRACES 2013 pSF_6/pCFC-11 versus pSF_6/pCFC-12 ratio ages.

For SF_6 the minimum concentration used is 0.04 fmol/kg and for CFC-11 and CFC-12 the minimum concentration used is 0.02 pmol/kg. These concentrations are greater than the minimum analytical errors (~3%) (Bullister et al. 2000). Contributing to the errors in tracer ages are: accuracy of the solubility measurements (1.5%, Warner and Weiss, 1985) and both diffusive and non-linear mixing (25%, Thiele and Sarmiento,

1990). The square root of the sum of the squares of the errors is ~27% for tracer ages (Fine et al., 2001).

The tracer ages presented in Table 1 have been averaged within layers and regions, due to the sparsity of the bottle data. Still there are layers throughout the regions, for example in the ODZ in layers 2 and 3, where there are ages are not determined due to low tracer concentrations.

3.2 *Oxygen Utilization Rates*

Oxygen concentrations will decrease due to mixing with waters having less oxygen and due to biological consumption. Apparent oxygen utilization (AOU) is the difference between oxygen gas solubility calculated from the in situ potential temperature and salinity and the measured oxygen concentration (Jenkins, 1977; Murray and Riley, 1969). Oxygen Utilization Rate is a measure of how fast oxygen is being consumed, determined from the slope between AOU and the tracer age (Jenkins, 1977). Jenkins points out that OUR is the upper limit of the true oxygen utilization rate.

$$\text{OUR} = \text{AOU}/\text{tracer age}$$

There are at least three methods that can be used to calculate OUR (Sonnerup et al., 2013). The isopycnal gradient method uses isopycnal gradients in AOU and ventilation age to calculate OUR_{grad}. The isopycnal advection and mixing method uses mass balances of isopycnal mixing, advection and in situ consumption to calculate $\text{OUR}_{\text{adv-diff}}$. The method used here is the path-integrated OUR, which uses AOU and the mean tracer age of the sample to calculate AOU_{path}. This method is chosen because of the availability of data for the needed parameters; temperature, salinity, dissolved oxygen, and transient tracers.

CTD oxygen measurements are estimated to have an error of 1-1.5% (Bullister et al., 2000). For AOU the error is estimated from the square root of the sum of the squares of the contributing terms (Wolberg, 1967), which are oxygen concentration and oxygen solubility. The error in oxygen solubility is estimated to be 0.3-0.7% (Weiss, 1970). The error for AOU is estimated to be 1.7%. The largest contribution to an uncertainty in OUR is due to errors in the tracer ages ~27% as evaluated above. Thus, the error in OUR is taken as ~30%.

3.3 *O_2* A Semi-Conservative Tracer*

Jenkins (1982) defined AOU as the "measurement or determination of those physical transport processes, coupled with observation of the oxygen distribution will lead to an estimate of the net oxygen utilization rate (OUR)." AOU in certain regions of the oceans (tropics) must be viewed with caution. Sarmiento and Gruber (2006) point out that in regions where the circulation is slow and AOU is large (e.g., tropical ODZs), it becomes difficult to determine how much of the large AOU signal is due to oxygen remineralization and how much is from the slow circulation. Therefore, attributing a large AOU in the tropics to remineralization could be overestimating biological process. For this reason, we choose to apply the O_2* method of Gruber et al. (2001) to estimate the biological component of observed oxygen changes.

The semi-conservative tracer O_2^* (Gruber et al., 2001) can be used to estimate changes over time in oxygen. The intention is to use O_2^* to differentiate between the physical and biological processes contributing to changes in oxygen when comparing datasets taken at different times and at similar locations. O_2^* is the difference between the measured oxygen concentration (O_2) and oxygen that is required, based on the

stoichiometry of the Redfield ratio ($r_{O2:PO4}$; Redfield, 1958, 1934), for the amount of phosphate (PO_4) that is in the sample (Gruber et al., 2001). O_2^* is calculated using the following equation.

$$O_2^* = O_2 - O_2^{*b}$$

$$O_2^{*b} = r_{O2:PO4} PO_4$$

The assumptions in the O_2^* method are that the circulation is known, biology affects O_2 and nutrients at a constant ratio, and there are no sources or sinks of O_2^*. Additionally, it is assumed that O_2 in the surface ocean equilibrates within a few days (Gruber et al., 2001). We are assuming that effects of denitrification are not impacting the oxygen distribution. Note that - most of these effects on nitrogen occur well east of 85°W and therefore east of our region of interest.

Further assumptions in the O_2^* method involve preformed phosphate, that is phosphate at the ocean surface when a water mass is subducted. PO_4 as measured includes preformed phosphate. The preformed PO_4 increases the O_2^* value by the amount of oxygen that is equivalent to the preformed concentration. In the South Pacific, the preformed PO_4 makes up ~50% of the measured PO_4, therefore the O_2^* is a much larger value than would be expected based on oxygen and AOU. However, we are assuming that the preformed portion remains constant on decadal timescales (Sarmiento and Gruber, 2006). Thus, the preformed PO_4 does not affect the terms used here as we are looking at differences between O_2^* and O_2^{*b}, i.e., the preformed values cancel out.

Henceforth, we refer to changes in oxygen represented by O_2^* as the contribution from physical processes, such as changes in circulation, ventilation, and stratification.

We refer to changes to interior oxygen represented by O_2^{*b} as the contribution from biological processes, which is due to the changes in phosphate concentrations and the Redfield ratio. Since the ratio of oxygen to phosphate is large, small changes in the phosphate concentration can equate to large changes in the O_2^* tracer. Thus, when there are changes in phosphate, the O_2^* tracer may not be useful, and for this reason the contribution from phosphate changes will be estimated. We estimate the uncertainty in O_2^{*b} using the method of Wolberg (1967). The error is equal to the square root of the sum of the squares of the (quasi-independent) terms contributing to O_2^{*b}, these are phosphate concentration (0.03 μmol/kg) and the Redfield ratio. Using an error of ±10 for the Redfield ratio from Anderson and Sarmiento (1994), we estimate the error for O_2^{*b} is ~10 μmol/kg.

The O_2^{*b} tracer includes biological processes via the Redfield ratio and carbon export calculated from the PO_4 concentration. Here we define the Beta O_2 method as an estimate of the year to year change in O_2^* and take it as an indicator of the difference between biological pump and physical changes to oxygen.

$$\Delta O_2^* = O_2^* \text{ (yr 2)} - O_2^* \text{ (yr 1) (and similarly for } \Delta O_2^{*b})$$

$$\Delta O_2^{*b} - \Delta O_2^* = \beta O_2$$

A positive Beta O_2 and is an indication that changes in the biological pump (ΔO_2^{*b}) are larger than changes in ventilation (ΔO_2^*). In the ODZ, we will find that Beta O_2 will be opposite in sign to changes in oxygen concentration. In general, where the O_2^* method is valid, Beta O_2 should be similar in value to changes in oxygen concentration. However, as we will see below (results section), they are not exactly the same. Reasons for the

small differences can be due variability in the Redfield ratio as discussed in the next section.

3.4 *Redfield Ratio Variability*

The $-O_2$:P Redfield ratio varies in the ocean (Redfield, 1958, 1934). In highly productive regions, such as the tropical Pacific Ocean, -175 is commonly used for the Redfield ratio (Keeling and Garcia, 2002). Anderson and Sarmiento (1994) find an $-O_2$:P ratio ranging from ~-150 to -200 for the global ocean. From this they conclude that an average $-O_2$:P ratio of -170 ± 10 can be used for the entire ocean below 400m. We calculated the negative of O_2:P ratios from 10ºN to 45ºS in the central and eastern Pacific using a linear fit of O_2 to P and only data in the density range of interest (26.5-27.0 σ_θ), which is centered around 400m. The ratio of O_2:P was calculated using a linear method and gives r^2 values >0.9. In the eastern South Pacific, the $-O_2$:P ratio varies from ~-150 in the subtropical gyre (at 150°W) to ~-195 in the ODZ (at 88°W) for data from the early 1990s. Due to the availability of data at 150°W and 103°W during all two decades, these two cruises were averaged. This gives an average value of -166 for the 1990s $-O_2$:P ratio and -178 for the 2000s/2010s. Data from the 2000s show an absolute increase in the ratio of ~12 in both the gyre and ODZ. This increase substantiates our assertion that the Redfield ratio should be estimated locally for specific regions rather than using an ocean average.

3.5 *Potential Vorticity*

Potential vorticity, Q, is used as a gauge of the stability of the water column and is derived from the Brunt-Vaisalla Frequency, N^2, Coriolis parameter, f, and gravity, g.

$$Q = f/g*N^2$$

An increase in potential vorticity implies an increase in stratification, less vertical mixing and a decrease in the vertical transport of oxygen. We use potential vorticity to compare stratification between the 1990s and 2013 data.

Chapter 4: **Results**

In this section we first examine oxygen parameters from the 2013 EPZT GEOTRACES data. Next, we compare GEOTRACES data to historical data by region: ODZ, boundary, and gyre.

4.1 ***GEOTRACES Oxygen Parameters***

First, the 2013 GEOTRACES data are used to examine the large-scale patterns of oxygen, AOU, ages and OUR. In Figure 4.1, the ODZ region in purple has concentrations close to 0 μmol/kg. Oxygen concentrations increase westward into the subtropical gyre and towards the ocean surface. Note that the cruise track is along the equatorward part of the subtropical gyre and oxygen concentrations are relatively low as compared with gyre waters further south and closer to sources. The ODZ is primarily between the Peru coast and 100ºW. Though oxygen concentrations exceed 50 μmol/kg, there is still a vertical minimum in oxygen concentrations extending into the gyre. In the boundary region between the ODZ and subtropical gyre, at 100ºW and 110ºW, the vertical minimum in the oxygen concentrations extends over a smaller part of the water column in density and depth space as compared with in the ODZ. Also, in the boundary region, oxygen concentrations greatly exceed 5 μmol/kg.

The pSF_6/pCFC-12 tracer ages are given in Table 1 (Appendix). Water in the ODZ in layer 1 has ages exceeding 21 years. The tracer ages show that ODZ water is older and suggest it cannot be affected by recent decadal ventilation changes at similar densities in the subtropical gyre (e.g., Fine et al., 2017). This observation is important for evaluating which processes affect oxygen parameters on decadal time scales.

AOU values for the 2013 GEOTRACES data (Fig. 4.2), show an increase from the surface through 27.2 σ_θ, and from the gyre eastward to the ODZ. The largest AOU values (~250 µmol/kg) are within the ODZ, and as expected are much smaller in the oligotrophic subtropical gyre (~175-200 µmol/kg).

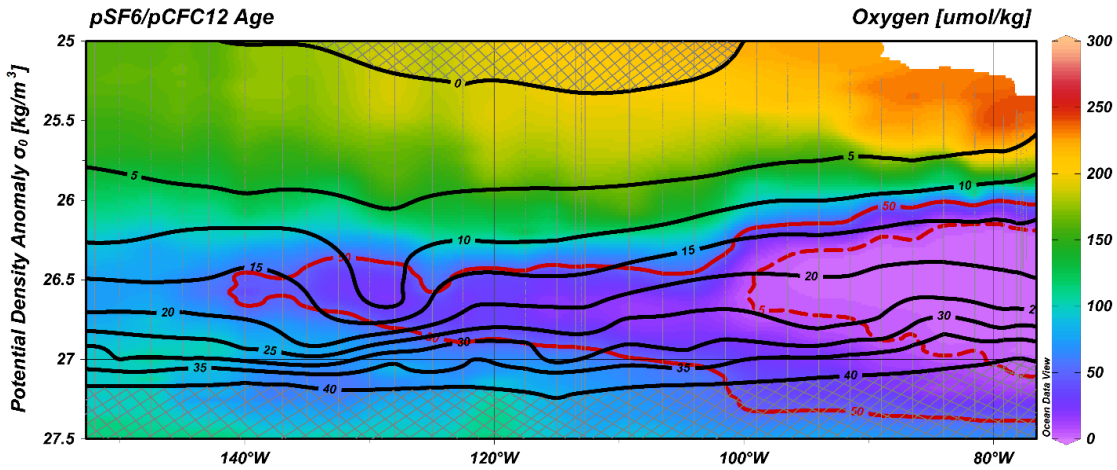

Figure 4.1. CTD Oxygen concentrations (µmol/kg) color bar on right from 0 to 300 µmol/kg with pSF_6/pCFC-12 age (years) contours in black across 2013 section of GEOTRACES EPZT. Solid red curve is the 50 µmol/kg oxygen contour, dashed red curve is the 5 µmol/kg oxygen contour. Note that this section extends over a larger density range than the figures below. Dashed vertical lines are locations of CTD casts. The hatching on top and bottom of the section refer to ages: upper is mixed layer, and lower has ages greater than 40 years and beyond the analytical capability.

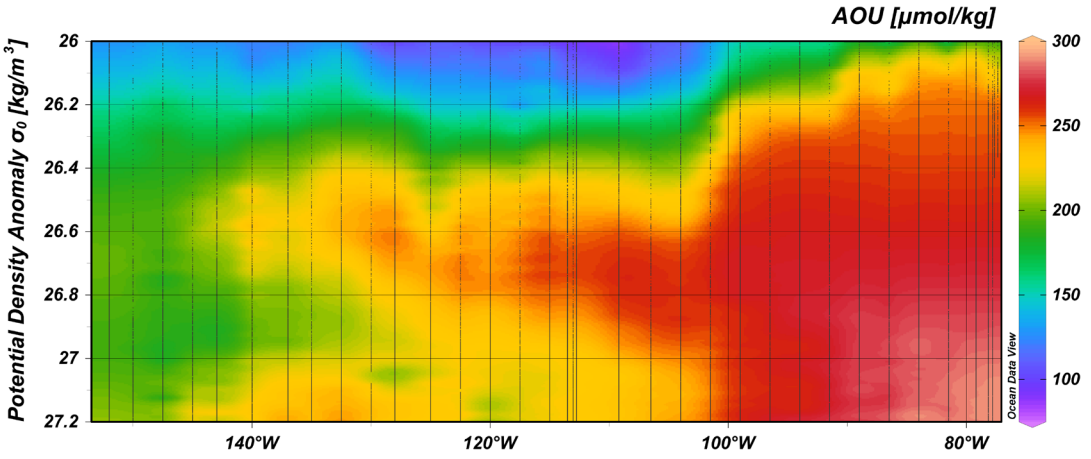

Figure 4.2. CTD AOU (µmol/kg) color bar on right from 0-300 µmol/kg across 2013 section of GEOTRACES EPZT. Dashed vertical lines indicate location of CTD casts.

4.2 *GEOTRACES and Historical Data*

Here we look at changes in oxygen parameters (O_2, AOU, PV) and averages (age, OUR) using data from the last few decades. We present the data in Tables 1 and 2 and comparisons by region (see Appendix).

4.3 *ODZ Region*

In the ODZ, select stations are compared from 2013 with 1990s data in the ODZ, specifically those within the black box of figure 2.1. Table 1 gives means and standard deviations, which are taken as the scatter in parameters within a layer as compared with the cruise mean for the layer. In layers 1 and 3, from 1993 to 2013 oxygen concentrations decrease and AOUs increase; however, the changes are within the standard deviations. In layer 2, over the same period oxygen concentrations decrease and AOUs increase a larger amount than the standard deviations and are thus significant. In addition, the 2013 data, oxygen concentrations are mostly less than 10 μmol/kg, whereas oxygen concentrations in the 1990s data are higher by ~5 μmol/kg and more variable (Figs. 4.3 and 4.4). Also, there is an extension of the <5 μmol/kg concentrations into deeper layers, which is an additional ~300 m (Fig. 4.4), This shows a vertical expansion of the lowest oxygen in the ODZ over time. The average oxygen in the whole layer 26.5 to 27 σ_θ decreases by ~5 μmol/kg (Figs. 4.1 and 4.4), and there is a similar increase in AOUs. In summary, in the layer of interest 26.5 to 27 σ_θ, there is a trend of decreasing oxygen and increasing AOU – although only in layer 2 are changes larger than the standard deviations.

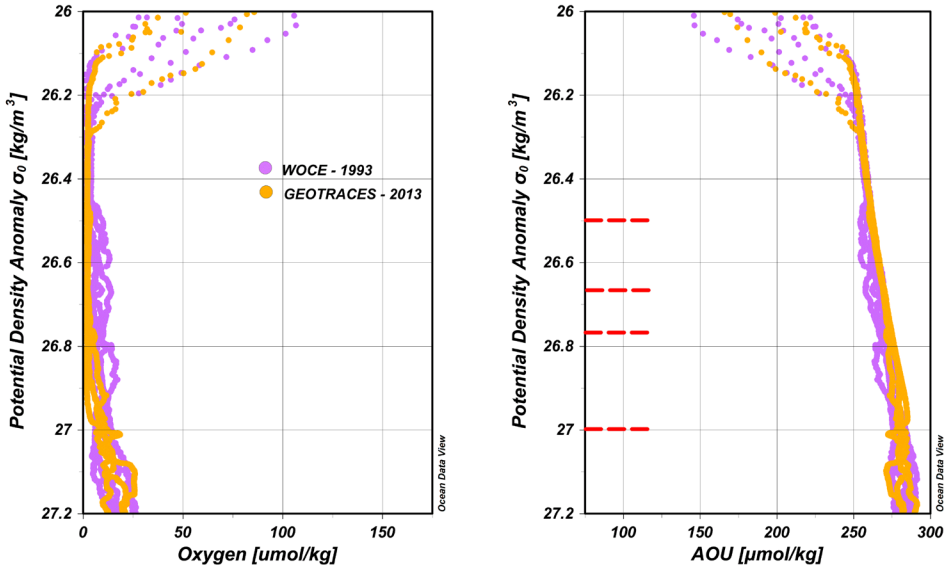

Figure 4.3. For ODZ region: A. CTD Oxygen concentration (µmol/kg) versus potential density anomaly (kg/m^3). B. CTD AOU (µmol/kg) versus potential density anomaly (kg/m^3). Red dashed lines show the density layers of interest.

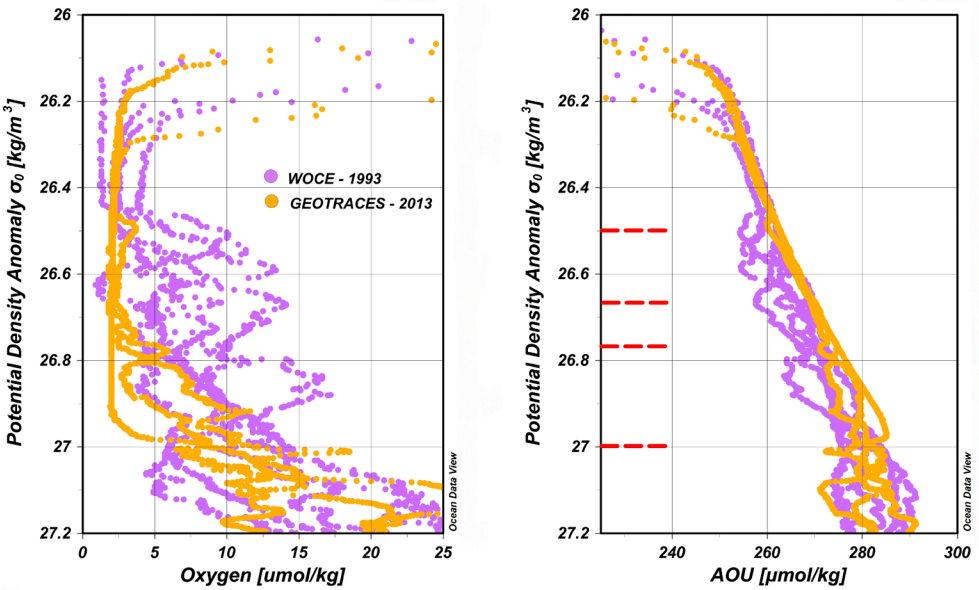

Figure 4.4. For ODZ: CTD Oxygen concentration from 0-25 µmol/kg versus density anomaly. CTD AOU from 220 to 300 µmol/kg versus density anomaly. Red dashed lines show the density layers of interest.

To help explain the observed changes in oxygen parameters, we examine hydrographic and nutrient data for trends within the three layers. Within 26.5 to 27.0 σ_θ, temperature, salinity, and phosphate do not change - within the error of the standard deviations and over the time period, 1990s-2013 (Table 1). Note that although Brewer and Peltzer (2017) found that 95% of oxygen consumption is driven by temperature due to the effect of temperature on microbial rates, this effect should not be significant over the small temperature changes observed in this study in all the regions.

To assess the contribution of biological processes to the trend of decreasing oxygen concentrations and increasing AOUs over two decades in the ODZ, we calculate O_2^* (see section 3.3). The O_2^* represents the change in ventilation and the O_2^{*b} represents the contribution to the change in oxygen from biological processes. Both O_2^* and O_2^{*b} increase monotonically from the 1990s to 2013 (Fig. 4.5). The differences between O_2* in 1993 and 2013 are larger than the estimated error of ~10 μmol/kg (section 3.3), the same applies to O_2^{*b}. The Beta O_2 method estimates the year to year change in oxygen calculated from Redfield ratio using phosphate. Throughout the ODZ Beta O_2 is positive. When Beta O_2 is positive, then biological processes dominate over physical processes as regards changing oxygen concentrations. Theoretically, Beta O_2 should be equal to changes in oxygen concentrations (Table 2). However, as discussed above (section 3.3) there may be small differences. In layers 1 and 3, Beta O_2 is larger than the decrease in oxygen concentrations - though within the standard deviations. In layer 2, Beta O_2 closely matches the decrease in oxygen concentrations. Thus, within the standard deviations of oxygen concentrations and Beta O_2, their values are in reasonable agreement. This is particularly the case in layer 2 where oxygen concentrations decrease significantly.

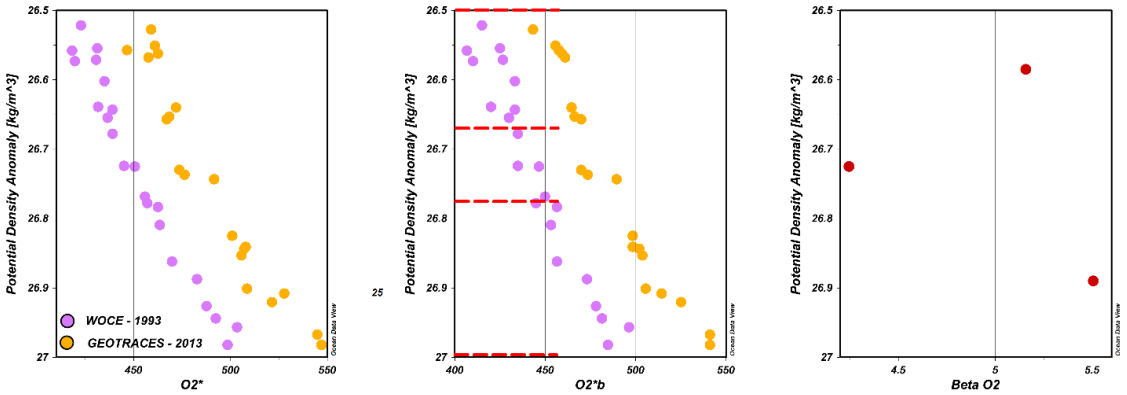

Figure 4.5. For ODZ region from 26.5 to 27 σ_θ three panels are: O_2^* (µmol/kg). O_2^{*b} (µmol/kg), and βO_2. As O_2* uses PO_4 the calculation requires bottle data. In the third panel, the three points βO_2 are an average for each layer.

Climate models suggest that as the ocean warms stratification will increase, which should inhibit vertical mixing of oxygen rich surface layers into the ODZ. Potential vorticity (Q) is used to gauge changes in stratification and stability of the water column, as a more stable water column will inhibit vertical mixing of oxygen. Between the top and bottom of our layer of interest, there is a trend of Q decreasing with depth. Although there is a lot of scatter in the CTD PV data, even after applying a moving average, there are no discernable trends. In the ODZ in all three layers, 1990s and 2013 stations show a large scatter in Q (Fig. 4.6). Thus, when comparing the mean of the 1990s stations to 2013 stations, within each layer, potential vorticity does not show significant changes that exceed the standard deviation of each cruise (Table 1). Thus, we conclude that changes in stratification are not likely affecting the observed changes in oxygen parameters.

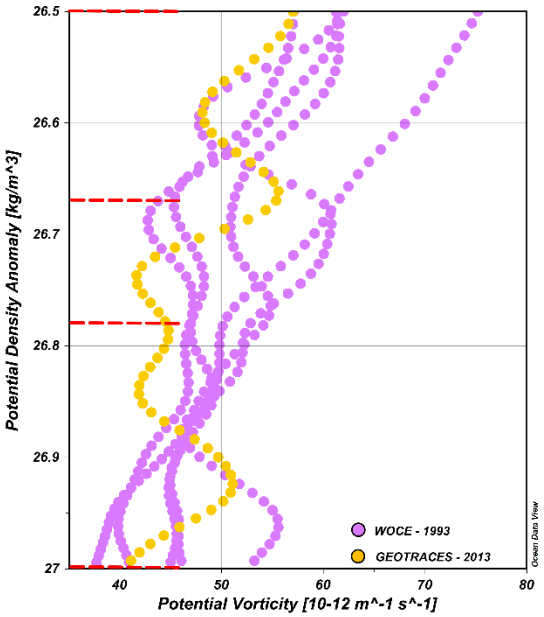

Figure 4.6. For the ODZ: smoothed Q in units 10^{-12} /m/s in the layer of interest. Note that 2013 data are in orange and the 1990s data are in purple. Red dashed lines show the density layers of interest.

Finally, in the ODZ there is ~300 m vertical expansion of the <5 µmol/kg contour between the 1990s and 2013. The <50 µmol/kg layer extends to ~27.36 σ_θ and ~960 m, and the vertical extent does not appear to change from 1990s to 2013. However, we cannot say with certainty whether there is southwestward spreading of the ODZ between the 1990s and 2013/2016. The ODZ contains 5 µmol/kg contour and the 50 µmol/kg contour extends between 26.2 to 27.3 σ_θ, thicker than to the west (Fig. 4.1). The southwest and northeast boundary regions (Figs. 1 and 5) usually contain the 50 µmol/kg contour, yet they do not contain the 5 µmol/kg contour. The northeast boundary contains the <50 µmol/kg contour, and thus seems to be within the ODZ over the decades. While the southwest boundary could be considered within the ODZ during 2013 and 2016, but not 1994. Czeschel et al. (2015) have shown a seasonal cycle in source currents implies a seasonal change in the amount of incoming oxygen. Both southwest and northeast

boundary stations had cruises occurring in different seasons. The southern boundary of the ODZ shifts in response to changes in the trade winds. It is southwestward in the summer and fall months with the weakening of the South Equatorial Countercurrent (SECC). In the winter and spring months the southern ODZ boundary shifts northeastward. These seasonal variations maybe superimposed on the long-term climate related decrease in oxygen content of the ODZ. Thus, we cannot conclude whether there is a significant, i.e., non- seasonal related southwestward spreading of the 50 μmol/kg contour.

In summary, the three layers of the ODZ show a trend of decreasing oxygen concentrations and increasing AOUs, which is however close to the standard deviations representing scatter in the data (Tables 1 and 2). The largest oxygen decrease occurs in layer 1, which is closest to the core of the ODZ. The most significant oxygen decrease occurs in layer 2. The O_2^{*b} indicates that decreasing oxygen concentrations between 1990s and 2013 are more affected by biological processes than by physical processes. Our results agree with Llanillo et al. (2018) who find that over the entire ODZ biological consumption - as compared with advective and diffusive fluxes – has a larger role in the oxygen decrease during the Argo period 2004-2012.

4.4 ***Boundary Region***

In the boundary region between the ODZ and the subtropical gyre, there were several repeat hydrography cruises around longitudes 100 to 110°W. As suggested by clustering of properties, (Fig. 2.3) the boundary region has been divided as follows. The northeast boundary region includes the stations northeast of the <50 μmol/kg 1990s oxygen contour (Fig. 2.1). The southwest boundary region includes stations that are

southwest and greater than the 50 μmol/kg oxygen concentration (Fig. 4.7). The division into northeast and southwest is in the same location for each of the three layers. The northeast boundary region has warmer and saltier water as compared with the southwest. The point of comparing the data over time in the boundary regions is to show that both boundary regions show similar changes in oxygen parameters to the ODZ.

4.4.1 *Northeast Boundary Region*

In the northeast boundary region and in all three layers, temperature varies within the standard deviation (Tables 1 and 2). In layers 1 and 2, oxygen concentrations decrease and AOUs increase significantly over the period 1994 to 2016. In layer 3, oxygen concentrations decrease and AOUs increase within the standard deviations. Note that in layer 3, from 2008 to 2016 there is no significant change in oxygen concentrations or AOUs. In summary, in the northeast boundary region, in layers 1 and 2 there is a significant decrease in oxygen concentrations and an increase in AOUs from 1994 to 2016. The largest oxygen decreases and AOU increases are observed in layer 1, followed by layer 2. In layer 3, decreases in oxygen concentrations and increases in AOUs are not significant.

4.4.2 *Southwest Boundary Region*

In the southwest boundary region and in all three layers, both temperature and salinity) show a small monotonic increase that is close to the standard deviations from 1994 to 2016, again not large enough to cause observed changes in oxygen. In all three layers, oxygen concentrations decrease and AOUs increase monotonically and significantly over the period 1994 to 2016 (Tables 1 and 2).

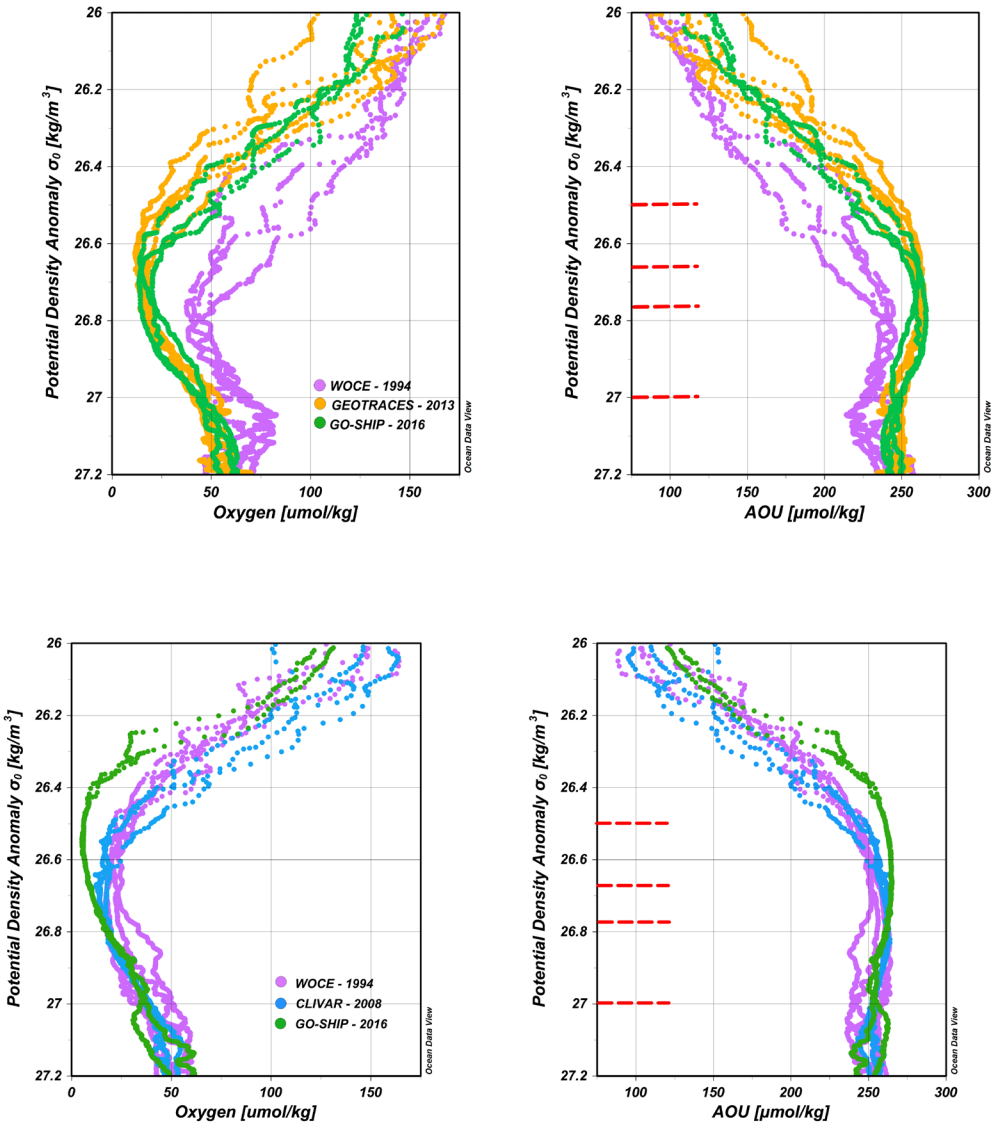

Figure 4.7. For southwest (top figures) and northeast boundaries (bottom figures): CTD oxygen (µmol/kg) versus potential density anomaly (kg/m^3). CTD AOU (µmol/kg) vs potential density anomaly (kg/m^3). Red dashed lines show the density layers of interest.

4.5 *East Gyre Region*

In the east gyre region, we are comparing stations within the black box (Fig. 2.1 and Fig. 4.8). In layers 1 and 2, although temperature increases are in the tenths of a degree (Tables 1 and 2), these increases will not change the oxygen saturations and

concentrations enough to affect the observed oxygen concentration changes. In layer 1, oxygen concentrations and AOU do not change within the standard deviations. In layer 2, oxygen concentration increases and AOU decreases are significant. In layer 3, temperature does not change within their standard deviations over the time period 1991 to 2013, and the salinity increases will not affect the oxygen saturations or concentration increases. Oxygen concentration increases and AOUs decreases are significant and exceed the standard deviations. In summary, in layers 2 and 3 of the east gyre, oxygen is increasing and AOU is decreasing, while in layer 1 there are no changes within the standard deviations. Also, in the east and central subtropical gyre regions, we were not able to use the O_2* method to assess biological contributions to oxygen changes as was done in the ODZ. The PO_4 in subtropical gyre changed, while in ODZ it remained constant within errors over the two decades. One of the perquisites to applying the Beta O2 method is a constant PO_4.

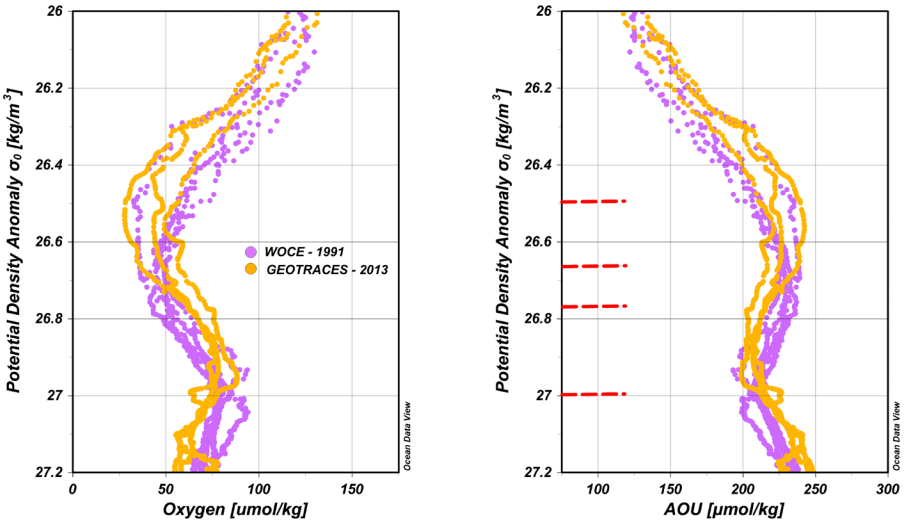

Figure 4.8. For the east gyre region from 26.5 – 27 σ_θ: A. Oxygen (µmol/kg) versus potential density anomaly (kg/m^3). B. AOU (µmol/kg) versus potential density anomaly (kg/m^3). Red dashed lines show the density layers of interest.

4.6 *Central Gyre Region*

For all the data between 1991 and 2015 there is a vertical minimum in oxygen concentration extending westward along 12°S from the ODZ to 150°W (Fig. 4.9). However, at 150°W oxygen concentrations are higher than the 50 μmol/kg threshold for the ODZ, and the vertical minimum extends over a smaller density range of only 26-27 σ_θ. In the central subtropical gyre, we are comparing stations within the black box (Fig. 2.1) and within the three layers. In all three layers, temperature is not monotonic and salinity varies by a small amount over the period 1991 to 2015 (Tables 1 and 2). These small T and S changes will not affect oxygen saturations and concentration increases. In all three layers, oxygen concentrations are similar within the standard deviations in three of the years: 1991, 2006 and 2015. Also, oxygen concentrations are significantly higher during 2013 as compared with the other three occupations, and correspondingly AOUs are lower (Tables 1 and 2). In summary, in the central gyre in all three layers in 1991, 2006 and 2015 oxygen concentrations and AOU are fairly constant. There is a significant increase in oxygen concentrations and decrease in AOU in all three layers in 2013 as compared with the other three occupations. In chapter 5, we discuss reasons for the observed changes.

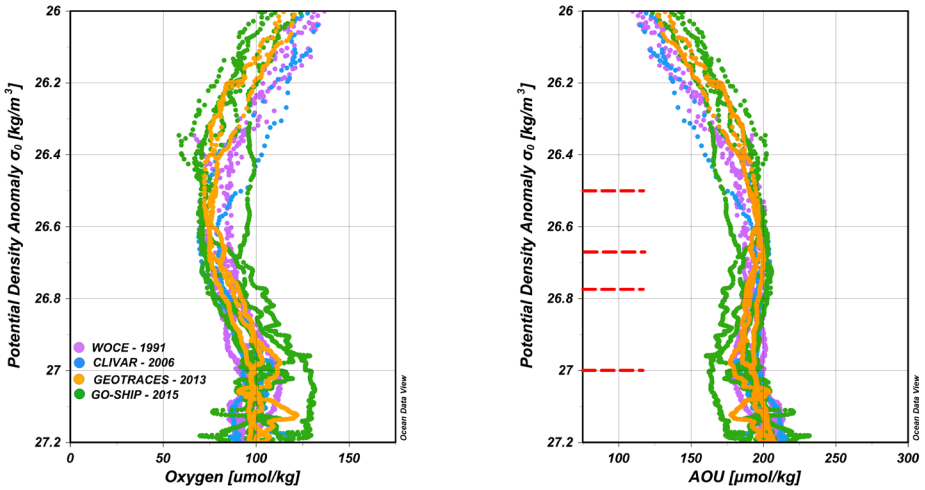

Figure 4.9. For central gyre region: CTD oxygen (µmol/kg) versus potential density anomaly (kg/m^3). CTD AOU (µmol/kg) vs potential density anomaly (kg/m^3). Red dashed lines show the density layers of interest.

4.7 *OUR*

The OUR is estimated as AOU divided by transient tracer age, and the age contributes most of the error. AOU is highest in the ODZ and decreases monotonically westward into the subtropical gyre. However, due to the sparsity of transient tracer observations (most layers only have several data points for tracers), OURs are presented together within regions and layers (Table 1). Although there is a trend of lower OUR with increasing depth, standard deviations and errors also suggest averaging the data. OURs in the ODZ are ~12 µmol/kg/yr and in the subtropical gyre regions they are 7-13 µmol/kg/yr. In the discussion section, we compare OURs from this study to earlier work.

Chapter 5: **Discussion**

We examine reasons for changes in oxygen concentrations and AOUs over two decades in the South Pacific ODZ and adjacent subtropical gyre. Also, we compare our results to earlier works. Though earlier works have documented changes in oxygen parameters in the South Pacific, in this discussion we are adding new detail and to an understanding of the processes causing the changes. The discussion is focused by region as different processes appear to dominate in the ODZ as compared with the subtropical gyre. In the lower thermocline, tracer age differences that can exceed 7 years (Table 1) suggest different renewal time scales from the water mass source regions for the ODZ and subtropical gyre. Based on renewal time scales, we will not be surprised to see that oxygen parameters in the two regions are changing differently over the two decades, and there are different processes dominating.

5.1 ***ODZ***

We are focusing on changes in oxygen parameters within the core of ODZ (<50 μmol/kg) over two decades of observations. The ODZ region shows a consistent trend of decreasing oxygen concentrations through the three layers. We examined changes in T and S as they can affect oxygen. However, within the standard deviations of the CTD measurements, T and S do not change over the two decades (Tables 1 and 2). This removes solubility differences as a factor affecting oxygen concentrations over the two decades. In the next sections we examine these changes in detail and discuss the rationale.

5.1.1 *Oxygen Changes*

Changes in oxygen concentrations within the ODZ core are compared to trends in earlier work from the equatorial Pacific, South Pacific and the North Pacific ODZs and the processes affecting the changes are examined. Several earlier works looking at changes in oxygen have concentrated on 10ºN to 10ºS; here, we are looking at the core of the South Pacific ODZ which is southward of these studies. Oxygen concentrations decrease in the ODZ, from 1993 to 2013 between 26.5 and 27 σ_θ (from ~200-500 m) by more than 50% (~3.7 μmol/kg) (Fig. 4.2, Tables 1 and 2). Our annual decrease of 0.19 ± 0.16 μmol/kg/yr is also larger than the annual decrease found by Stramma et al. (2008) of 0.13 ± 0.32 μmol/kg/yr from 1960-2008 at 300-700 m. The Stramma et al. results are from a region of 5ºN to 5ºS and 105º to 115ºW, which is north and west of the region analyzed here. The regions closer to the equator are influenced more by the relatively oxygen rich South Equatorial Countercurrent, which could lessen some of the oxygen decrease we find in the ODZ. Also, our data were taken another five years after those of Stramma et al. Thus, differences between their and our work could be due to short-term trends. Stramma et al. find a long-term trend of decreasing oxygen starting in 1960. A recent study by Ito et al. (2017) finds that the South Pacific ODZ core at 400 m is among those regions with the weakest oxygen trends in the entire ocean much less than 0.1μmol/kg/yr. Their depth of 400 m is at the deeper part of our layer of interest, still though their trend is smaller than our results, it is within our standard deviation.

5.1.2 *AOU Changes*

In correlation with the decrease in oxygen concentrations in the ODZ over two decades, we find that AOUs increase from 1993 to 2013 between 26.5 and 27 σ_θ. The

AOU increase is about the same magnitude, ~5 μmol/kg, as the decrease in oxygen concentrations. In the North Pacific ODZ from 26.2 to 26.4 σ_θ where oxygen is <50 μmol/kg, Sonnerup et al. (1999) estimate from 1991 data an AOU of ~200-225 μmol/kg at ~10ºN and 150ºW. Theirs is smaller than our AOUs of ~260-275 μmol/kg, in the South Pacific ODZ where oxygen is also <50 μmol/kg. The differences could be due to regional differences and temporal variability in the winds.

The processes affecting changes in AOU can be several. These can include changes in temperature and stratification (e.g., Gnanadesikan et al., 2007), which we discuss in the above section 4 are small. They also can include changes in ventilation e.g., due to changes in the southern hemisphere westerly winds (Southern Annular Mode, SAM) (e.g., Fine et al., 2017). Waters become greatly diluted after leaving the source region due to their long path into the ODZ. As the ages in the ODZ exceed two decades (Fig. 2.4, Table 1), changes in the SAM are also not likely to influence AOU changes between mid-1990s and 2013. Supporting this assertion are the Llanillo et al. (2018) results. They find that the tropical versus subtropical water contribution to the South Pacific ODZ is in a ratio of 2:1. When they further subdivide the subtropical contribution into that from the Peru-Chile countercurrent and subtropical waters they find the countercurrent contribution varies from ~50-30%. Their results show that the small percentage of subtropical water in the ODZ is diluted by tropical and upwelled coastal waters.

Our calculations (chapter 4) of $O_2{}^{*b}$ for the ODZ suggest that the major reason for decreasing oxygen concentrations and increasing AOUs between the 1990s and 2013 is due to the effects of increased biological as compared with physical processes. Earlier

work suggests that fluctuations in the trade winds could lead to a cycle of expansion and contraction of the North Pacific ODZ, and when trade winds decrease there is weaker coastal upwelling consistent with decreased AOU due to biological processes (Deutsch et al., 2014; McGregor et al., 2014). Climate models predict that increased warming will decrease - the trade winds, circulation (Vecchi et al., 2006) and upwelling. This decrease in the trades should lead to a decrease in AOU. However, we find an increase in AOU, which is consistent with a strengthening in the Pacific southeast trade winds starting in the 1990s that developed in addition to recent warming (Merrifield, 2011). Note that the trade winds decreased again in 2011 (Cha et al., 2018) - as expected from climate warming.

5.1.3 ***OUR***

Due to the sparsity of tracer data, we cannot make OUR comparisons between 1990s and 2013 data. Rather, we average ages for a region and our layer of interest. Most previous studies that have estimated OUR within ODZs find an exponential decrease between the euphotic zone and ~500 m. In our upper layer of the ODZ, the 1990s and 2013 average OURs are 12 μmol/kg/yr (~25% uncertainty). Karstensen et al. (2008) find an OUR range of 4-10 μmol/kg/yr (20% uncertainty) within the North and South Pacific ODZs from 1992 to 2001. They use CFC-11 and ^{14}C tracer ages in waters from 100-500 m and climatological mean averaged oxygen data. In the South Pacific ODZ, Llanillo et al. (2018) use three independent estimates of OUR: vertical velocity from the assimilative ocean model SODA, Karstensen et al.'s (2008) empirical expression for waters below 100 m for the entire Pacific Ocean, and deduced from Czeschel et al.'s (2015) oxygen float measurements below the seasonal thermocline. In density range of our upper layer,

Llanillo et al. results estimate OUR of ~7 μmol/kg/yr. Sonnerup et al. (2019) do not provide OURs from their observations, which are in the area offsore the Peru and Chile coastal upwelling. The OURs presented here are higher than these earlier studies. As pointed out by Sonnerup et al. (2013) our higher OURs could be due to the effects of mixing on the tracer ages. At present, we have no other explanations for our higher OURs except that they are consistent with our finding of increased biological processes causing decreased oxygen concentrations over the two decades.

5.2 ***Subtropical Gyre***

The large-scale oxygen distribution (Fig. 3.1) shows oxygen increasing nearly monotonically from the ODZ westward into the equatorward part of the subtropical gyre. In the layer of interest and in the 2013 and 1990s data, at about 135-137°W there is a horizontal oxygen minimum. There is also higher salinity at these longitudes (not shown). As we will show, even though the 2013 section of oxygen shows a horizontal minimum and higher salinity at 135-137°W in the gyre - still, when looking at changes from the 1990s to 2013 oxygen concentrations are mostly increasing.

5.2.1 ***Oxygen Changes***

There are substantial increases in oxygen concentrations in the central (10-20 μmol/kg) and less in east (<20 μmol/kg) gyre regions, in all three layers between the 1990s/2006 and 2013. (Note that as discussed above (chapter 4) changes in temperature and salinity are not enough to account for increases in oxygen.) The oxygen trends across the years are observed in the bottle and CTD oxygen data, and in most of the layers. Also, the oxygen trends from 1990s to 2013 are consistent with what others have published for

the South Pacific subtropical gyre. Roemmich et al. (2016, 2007) show a circulation increase in the South Pacific with an increase in southern hemisphere westerly winds starting in mid-1990s and continuing through 2014. Several earlier studies, using data from the central South Pacific subtropical gyre, have attributed increases in ventilation to changes in southern winds (e.g., Fine, 2011; Waugh et al., 2013; Fine et al., 2017). In 2015, oxygen concentrations decrease again to near 2006 concentrations in the central gyre. Decreasing oxygen concentrations in 2015 could also be related to changes in southern winds, though considering lag times of several years this cannot be substantiated as regards ventilation effects at present.

5.2.2 ***AOU Changes***

As compared with the ODZ, in the subtropical gyre AOU is nearly 100 μmol/kg lower (Table 1). AOU ranges from ~170-195 μmol/kg across the gyre regions. Consistent with the oxygen concentration increases, between 1990s and 2013, we find AOU decreases in all 3 layers and both gyre regions, though more substantially in the central gyre. Again, in the 2015 data from the central gyre, AOU increases to pre-2013 levels. Fine et al. (2017) also found decreasing AOU in the South Pacific subtropical gyre from the 1990s to 2000s data.

5.2.3 ***OUR***

We estimate that OURs in the subtropical gyre regions are 7-13 μmol/kg/yr across all three layers and cruises 1990s to 2016 (Table 1). Mecking et al. (2006), estimated an OUR of ~5.5-5.8 μmol/kg/yr along 152ºW at ~25ºS, from 26.45 to 26.65 σ_θ using pCFC-12 ages and data from 1991 and 1997. Given that the Mecking et al. results are from

further south and more into the middle of the gyre, it is not surprising that their OURs are at the low end of our range of OURs. Karstensen et al. (2008) estimated an OUR of 5-6 μmol/kg/yr at 152ºW from 23-35ºN in the North Pacific from 26.45 to 26.65 σ_θ. Similar to Mecking et al., Karstensen et al. OURs are from a region in the middle of the North Pacific subtropical gyre, a region that is more oligotrophic than the tropical region of our study. Sonnerup et al. (2015) found an OUR range of 8-20 μmol/kg/yr at 200 m, decreasing to 2 μmol/kg/yr at 500 m in 2007/8 along 103ºW from 30ºN to 70ºS. In the region from 30-42ºS along 103ºW, Sonnerup et al. found OURs ranging from 1.7-2.7 μmol/kg/yr from 26.5-27 σ_θ. Since the South Pacific is the most oligotrophic of the subtropical gyres, it follows that OURs from closer to the water mass sources should be smaller than we estimate for the region of 12°S. However, as in the ODZ, it is possible that our OURs are higher due to the effects of mixing on tracer ages (Sonnerup et al., 2019), and temporal variability.

5.3 ***Conclusions***

The 2013 GEOTRACES oxygen parameters along ~12°S from the ODZ to the South Pacific subtropical gyre are compared to 1990s WOCE and 2000s CLIVAR and 2010s Go-Ship data. We concentrate on the density range of well-ventilated SAMW, 26.5 to 27.0 σ_θ. The density is at the core of the ODZ. Here, we are assuming that pathways of water into the ODZ remained constant over the two decades, also that seasonal differences in cruises are not affecting differences in oxygen parameters in the lower thermocline. Differences in oxygen parameters in the ODZ and equatorward part of the gyre do not show the expected anthropogenic trend of decreasing oxygen or increasing AOU. In the ODZ, oxygen concentrations show a trend of decreasing from 1990s to 2013

and AOU increasing. In the ODZ, transient tracer ages in 2013 are relatively older ~23 years and the time scales for renewal by subtropical gyre waters is considerably longer due to longer pathways from source regions. We use the O_2* method of Gruber et al. (2001) to estimate the contribution of biological processes to the ODZ oxygen decrease. The method suggests that the trend of decreasing ODZ oxygen concentrations over two decades is due more to biological processes than physical processes. Our result is consistent with what is known about wind forcing in the tropics over these decades. Since the mid-1990s there has been an increase in trade winds (McGregor et al., 2014; Merrifield and Maltrud, 2011), and increased upwelling. Note the increase in trade winds is opposite to that predicted by models for climate warming. The proximity of the ODZ to coastal upwelling and increased upwelling are consistent with our observed trend of oxygen concentration decreases between 1990s and 2013. Our averaged OURs show higher rates in the ODZ and subtropical gyre than earlier studies, due mostly to geographic and time differences in OURs from earlier studies, and biases due to the effects of mixing on tracer ages.

In the equatorward part of the subtropical gyre on the other hand, over the two decades oxygen concentrations increased and AOU decreased between the 1990s and 2013. The increased ventilation of the South Pacific subtropical gyre related to an increase in southern hemisphere westerly winds (Roemmich et al., 2016, 2007) has been discussed in earlier works (e.g., Fine, 2011; Waugh et al., 2013; Fine et al., 2017). Though Roemmich et al. correlate the increased winds with increased ocean heat, they do not draw conclusions about the increased winds being due to long term climate change.

There is different wind forcing dominating the South Pacific ODZ and subtropical gyre: ODZ by tropical southeast trade winds, while gyre by westerly winds. During the past two decades, the different forcing's have resulted in oxygen parameters that are varying independently in ODZ and gyre. The effect of the westerly winds on ventilation is felt relatively quickly (of the order few years) in the subtropical gyre due to the proximity to water mass source regions, and these waters eventually are transported into the ODZ. However, their time scales for transport into the ODZ are long (of the order decades) and there is extensive mixing. One way the trades affect the ODZ is by changing the strength of coastal upwelling. In the ODZ, there are complex tradeoffs between biological demand related to changes in coastal upwelling versus changes in stratification and winds related to climate warming. Thus, differences in ages of the waters and time scales for transport from water mass source regions, proximity of ODZ to coastal upwelling and of the gyre to source regions, all suggest that the ODZ and gyre oxygen parameters may continue to vary independently in the two regions. It remains to be observed as the climate change signal strengthens affecting wind systems and stratification, whether oxygen parameters in the two regions – ODZ and subtropical gyre – may start to vary in synchronization with each other. Additionally, it will be useful to compare these results in the South Pacific, the most oligotrophic of the subtropical gyres, to their adjacent ODZs in the Atlantic and North Pacific. Continued global observations of gases that are critical to life, such as oxygen, are needed.

APPENDIX

	ODZ	
Latitude	11 - 13 °S	
Longitude	84 - 89 °W	
	March 1993	December 2013
26.5-26.67	210-335m	190-325m
Temperature	11.30 ± 0.35	11.30 ± 0.35
Salinity	34.818 ± 0.022	34.813 ± 0.023
Oxygen	6.5 ± 3.2	2.8 ± 0.5
O_2 % sat	2.4%	1.0%
AOU	261.7 ± 3.8	265.5 ± 2.4
PO_4	2.54 ± 0.06	2.58 ± 0.05
O_2*[b]	422.2 ± 9.9	459.7 ± 8.2
O_2*	429.4 ± 7.5	461.8 ± 7.8
Ratio Age	21	23 ± 4
OUR	12.5	11.8 ± 1.9
Q	57.3 ± 7.3	52.5 ± 3.1
26.67-26.78	300-400m	285-385m
Temperature	10.26 ± 0.27	10.22 ± 0.26
Salinity	34.750 ± 0.019	34.743 ± 0.018
Oxygen	7.1 ± 2.8	3.3 ± 1.1
O_2 % sat	2.6%	1.2%
AOU	267.3 ± 3.3	271.6 ± 1.7
PO_4	2.66 ± 0.04	2.69 ± 0.05
O_2*[b]	442.2 ± 6.9	478.4 ± 8.6
O_2*	449.5 ± 7.5	481.5 ± 8.1
Ratio Age	-	-
OUR	-	-
Q	51.8 ± 5.6	45.6 ± 4.3

26.78-27	360-555m	350-525m
Temperature	8.83 ± 0.56	8.80 ± 0.56
Salinity	34.664 ± 0.033	34.655 ± 0.033
Oxygen	9.6 ± 3.2	6.9 ± 3.7
O_2 % sat	3.4%	2.4%
AOU	273.9 ± 4.1	277.8 ± 3.3
PO_4	2.85 ± 0.09	2.89 ± 0.10
O_2*[b]	472.5 ± 15.7	514.4 ± 17.3
O_2*	482.5 ± 15.8	519.0 ± 17.4
Ratio Age	-	-
OUR	-	-
Q	46.3 ± 4.2	45.5 ± 3.4

	Boundary SW		
Latitude	14.5 - 16.5 °S		
Longitude	101.5 - 106.5 °W		
	April 1994	November 2013	December 2016
26.5-26.67	305-345m	295-350m	295-355m
Temperature	10.15 ± 0.35	10.42 ± 0.26	10.52 ± 0.30
Salinity	34.558 ± 0.023	34.618 ± 0.027	34.641 ± 0.020
Oxygen	66.8 ± 15.1	26.1 ± 9.4	19.1 ± 7.5
O_2 % sat	24.3%	9.5%	7.0%
AOU	208.6 ± 15.3	247.3 ± 10.3	254.0 ± 8.1
Ratio Age	-	24 ± 5	22.7 ± 0.2
OUR	-	11.0 ± 1.8	11.5 ± 0.01
26.67-26.78	335-375m	345-400m	330-390m
Temperature	9.36 ± 0.19	9.63 ± 0.23	9.66 ± 0.22
Salinity	34.559 ± 0.014	34.625 ± 0.015	34.626 ± 0.012
Oxygen	50.1 ± 9.8	20.8 ± 3.6	16.5 ± 1.8
O_2 % sat	17.9%	7.5%	5.9%
AOU	230.1 ± 10.0	257.6 ± 3.4	261.7 ± 1.7
Ratio Age	22.1	28 ± 1	25.6 ± 2.2
OUR	10.7	9.3 ± 0.2	10.2 ± 0.9
26.78-27	370-495m	380-515m	375-515m
Temperature	8.10 ± 0.49	8.28 ± 0.50	8.34 ± 0.51
Salinity	34.539 ± 0.018	34.576 ± 0.024	34.582 ± 0.020
Oxygen	52.3 ± 7.4	40.3 ± 10.7	33.8 ± 9.7
O_2 % sat	18.1%	14.0%	11.8%
AOU	236.2 ± 4.9	246.9 ± 8.6	253.0 ± 6.6
Ratio Age	26.4	-	23.7 ± 7.1
OUR	9.1	-	11.4 ± 3.2

	Boundary NE		
Latitude	13.5 - 15 °S		
Longitude	103 °W		
	April 1994	January 2008	December 2016
26.5-26.67	280-350m	285-335m	275-325m
Temperature	10.74 ± 0.34	10.61 ± 0.29	10.92 ± 0.31
Salinity	34.690 ± 0.020	34.654 ± 0.017	34.732 ± 0.011
Oxygen	23.0 ± 3.0	19.8 ± 5.7	6.7 ± 1.0
O_2 % sat	8.5%	7.3%	2.5%
AOU	248.5 ± 4.2	252.8 ± 6.6	263.9 ± 1.1
Ratio Age	23.5	15.4 ± 3.9	23.3
OUR	11	17.2 ± 4.4	11.2
26.67-26.78	330-395m	330-375m	325-375m
Temperature	9.81 ± 0.24	9.73 ± 0.25	9.96 ± 0.24
Salinity	34.661 ± 0.018	34.643 ± 0.013	34.697 ± 0.008
Oxygen	22.2 ± 3.6	16.0 ± 1.9	12.9 ± 2.4
O_2 % sat	8.0%	5.8%	4.7%
AOU	255.1 ± 3.9	261.8 ± 1.2	263.4 ± 1.0
Ratio Age	25.1 ± 1.5	-	31.2 ± 2.9
OUR	10.3 ± 1.0	-	8.4 ± 0.8
26.78-27	365-500m	370-500m	370-520m
Temperature	8.53 ± 0.51	8.42 ± 0.50	8.66 ± 0.53
Salinity	34.617 ± 0.027	34.596 ± 0.021	34.641 ± 0.026
Oxygen	34.6 ± 9.2	28.1 ± 6.6	29.0 ± 6.2
O_2 % sat	12.1%	9.8%	10.2%
AOU	250.7 ± 8.5	258.2 ± 3.3	255.6 ± 3.1
Ratio Age	28.5 ± 3.1	21.9	27.9
OUR	8.9 ± 0.5	12	9.1

	Central Gyre			
Latitude	9.5 - 11.5 °S			
Longitude	147.5 - 152 °W			
	September 1991	February 2006	December 2013	April 2015
26.5-26.67	325-390m	325-360m	320-380m	315-415m
Temperature	10.89 ± 0.46	11.00 ± 0.37	10.83 ± 0.34	10.81 ± 0.33
Salinity	34.724 ± 0.058	34.733 ± 0.021	34.703 ± 0.016	34.717 ± 0.026
Oxygen	79.2 ± 5.9	77.9 ± 6.9	90.2 ± 4.3	77.8 ± 9.8
O_2 % sat	29.3%	28.8%	33.2%	28.7%
AOU	191.6 ± 6.4	192.1 ± 8.0	181.2 ± 3.2	193.5 ± 9.4
Ratio Age	-	-	16 ± 1	18
OUR	-	-	12.6 ± 0.7	10.4
26.67-26.78	345-410m	350-380m	345-405m	345-440m
Temperature	9.93 ± 0.29	9.90 ± 0.23	9.92 ± 0.22	9.98 ± 0.24
Salinity	34.681 ± 0.042	34.685 ± 0.011	34.681 ± 0.012	34.688 ± 0.022
Oxygen	82.5 ± 5	76.8 ± 4.2	100.3 ± 7.7	83.4 ± 10.3
O_2 % sat	29.9%	27.8%	36.2%	30.2%
AOU	193.7 ± 4.9	199.9 ± 3.7	176.7 ± 6.9	192.9 ± 10.21
Ratio Age	-	-	21 ± 3	19
OUR	-	-	8.9 ± 1	10.4
26.78-27.00	365-530m	365-480m	370-515m	370-550m
Temperature	8.52 ± 0.52	8.49 ± 0.52	8.58 ± 0.51	8.56 ± 0.56
Salinity	34.626 ± 0.029	34.630 ± 0.023	34.631 ± 0.024	34.630 ± 0.031
Oxygen	92.1 ± 6.7	93.8 ± 7.2	113.9 ± 8.3	100.325 ± 13.0
O_2 % sat	32.3%	32.8%	39.8%	35.2%
AOU	193.5 ± 5.8	191.9 ± 5.3	172.1 ± 6.4	185.02 ± 11.5
Ratio Age	25 ± 4	-	-	22 ± 0.3
OUR	6.9	-	-	8.3 ± 0.8

	East Gyre	
Latitude	10.5 -12.5 °S	
Longitude	132.5 - 137 °W	
	July 1991	December 2013
26.5-26.67	310-390m	315-380m
Temperature	10.53 ± 0.41	10.89 ± 0.31
Salinity	34.648 ± 0.053	34.716 ± 0.017
Oxygen	48.7 ± 7.6	49.7 ± 9.7
O_2 % sat	17.8%	18.4%
AOU	224.3 ± 8.2	220.7 ± 9.0
Ratio Age	-	19
OUR	-	11.6
26.67-26.78	345-430m	345-410m
Temperature	9.73 ± 0.25	10.00 ± 0.22
Salinity	34.635 ± 0.040	34.700 ± 0.011
Oxygen	47.5 ± 5.4	75.0 ± 6.6
O_2 % sat	17.1%	27.2%
AOU	230.3 ± 4.9	201.5 ± 5.4
Ratio Age	-	-
OUR	-	-
26.78-27.00	375-530m	375-530m
Temperature	8.53 ± 0.47	8.57 ± 0.52
Salinity	34.623 ± 0.019	34.639 ± 0.025
Oxygen	70.7 ± 10.7	89.3 ± 6.0
O_2 % sat	24.8%	31.3%
AOU	214.0 ± 8.4	195.9 ± 7.3
Ratio Age	18 ± 2	-
OUR	12.0 ± 1.5	-

Table 1. Average properties for each region within layers and by cruise. Standard deviations are from the layer mean for that property.

	ODZ
Latitude	11 - 13 °S
Longitude	84 - 89 °W
	2013-1993
26.5-26.67	
Temperature	0 ± 0.35
Salinity	-0.005 ± 0.023
Oxygen	-3.7 ± 3.2
O2 % sat	-3.4%
AOU	3.8 ± 3.8
PO4	0.04 ± 0.06
$O2^{*B}$	37.5 ± 9.9
O2*	32.4 ± 7.8
Q	-4.8 ± 7.3
26.67-26.78	
Temperature	-0.04 ± 0.27
Salinity	-0.007 ± 0.019
Oxygen	-3.8 ± 2.8
O2 % sat	-1.4%
AOU	4.3 ± 3.3
PO4	0.03 ± 0.05
$O2^{*B}$	36.2 ± 8.6
O2*	32 ± 8.1
Q	-6.2 ± 5.6
26.78-27	
Temperature	-0.03 ± 0.56
Salinity	-0.009 ± 0.033
Oxygen	-2.7 ± 3.7
O2 % sat	-1.0%
AOU	3.9 ± 4.1
PO4	0.04 ± 0.10
$O2^{*B}$	41.9 ± 17.3
O2*	36.5 ± 17.4
Q	-0.8 ± 4.2

	Boundary SW		
Latitude	14.5 - 16.5 °S		
Longitude	101.5 - 106.5 °W		
	2016-1994	2013-1994	2016-2013
26.5-26.67			
Temperature	0.37 ± 0.35	0.27 ± 0.35	0.01 ± 0.30
Salinity	0.083 ± 0.023	0.060 ± 0.027	0.023 ± 0.027
Oxygen	-47.7 ± 15.1	-40.7 ± 15.1	-7.0 ± 9.4
Oxygen Sat	-17.3%	-14.8%	-2.5%
AOU	45.4 ± 15.3	38.7 ± 15.3	6.7 ± 9.4
26.67-26.78			
Temperature	0.30 ± -.22	0.27 ± 0.23	0.023 ± 0.23
Salinity	0.067 ± 0.014	0.066 ± 0.015	0.001 ± 0.015
Oxygen	-33.6 ± 9.8	-29.3 ± 9.8	-4.3 ± 0.015
Oxygen Sat	-12.0%	-10.4%	-1.6%
AOU	31.6 ± 10.0	27.5 ± 10.0	4.1 ± 3.4
26.78-27			
Temperature	0.24 ± 0.51	0.18 ± 0.50	0.06 ± 0.51
Salinity	0.043 ± 0.020	0.037 ± 0.024	0.006 ± 0.024
Oxygen	-18.5 ± 9.7	-12.0 ± 10.7	-6.5 ± 10.7
Oxygen Sat	-6.3%	-4.1%	-2.2%
AOU	16.8 ± 6.6	10.7 ± 8.6	6.1 ± 8.6

	Boundary NE		
Latitude	13.5 - 15 °S		
Longitude	103 °W		
	2016-1994	2008-1994	2016-2008
26.5-26.67			
Temperature	0.18 ± 0.34	-0.13 ± 0.34	0.31 ± 0.31
Salinity	0.042 ± 0.020	-0.036 ± 0.020	0.078 ± 0.017
Oxygen	-16.3 ± 6.7	-3.2 ± 5.7	-13.1 ± 5.7
Oxygen Sat	-6.0%	-1.2%	-4.8%
AOU	15.4 ± 4.2	4.3 ± 6.6	11.1 ± 6.6
26.67-26.78			
Temperature	0.15 ± 0.25	-0.08 ± 0.25	0.23 ± 0.25
Salinity	0.036 ± 0.027	-0.018 ± 0.018	0.054 ± 0.017
Oxygen	-9.3 ± 3.6	-6.2 ± 3.6	-3.1 ± 6.6
Oxygen Sat	-3.3%	-2.2%	-1.1%
AOU	8.3 ± 3.9	6.7 ± 3.9	1.6 ± 1.2
26.78-27			
Temperature	0.13 ± 0.53	-0.11 ± 0.51	0.24 ± 0.53
Salinity	0.024 ± 0.027	-0.021 ± 0.027	0.045 ± 0.026
Oxygen	-5.6 ± 9.2	-6.5 ± 9.2	0.9 ± 6.6
Oxygen Sat	-1.9%	-2.3%	0.4%
AOU	4.9 ± 8.5	7.5 ± 8.5	-2.6 ± 3.3

	Central Gyre				**East Gyre**
Latitude	9.5 - 11.5 °S				10.5 -12.5 °S
Longitude	147.5 - 152 °W				132.5 - 137 °W
	2013-1991	2006-1991	2013-2006	2015-2013	2013-1991
26.5-26.67					
Temperature	-0.06 ± 0.46	0.11 ± 0.46	-0.17 ± 0.37	-0.02 ± 0.34	0.36 ± 0.41
Salinity	-0.021 ± 0.058	0.009 ± 0.058	-0.03 ± 0.021	0.014 ± 0.026	0.068 ± 0.053
Oxygen	11.0 ± 5.9	-1.3 ± 6.9	12.3 ± 6.9	-12.4 ± 9.8	1.0 ± 9.7
O2 % sat	3.9%	-0.5%	4.4%	-4.5%	0.6%
AOU	-10.4 ± 6.4	0.5 ± 8.0	-10.9 ± 8.0	12.3 ± 9.4	-3.6 ± 9.0
26.67-26.78					
Temperature	-0.01 ± 0.29	-0.03 ± 0.29	0.02 ± 0.23	0.06 ± 0.24	0.27 ± 0.25
Salinity	0.000 ± 0.042	0.004 ± 0.042	-0.004 ± 0.012	0.007 ± 0.022	0.065 ± 0.040
Oxygen	17.8 ± 7.7	-5.7 ± 5.0	23.5 ± 7.7	-16.9 ± 10.3	27.5 ± 6.6
O2 % sat	6.3%	-2.1%	8.4%	-6.0%	10.1%
AOU	-17.0 ± 6.9	6.2 ± 4.9	-23.2 ± 6.9	16.2 ± 10.2	-28.8 ± 5.4
26.78-27					
Temperature	0.06 ± 0.52	-0.03 ± 0.52	0.09 ± 0.52	-0.02 ± 0.56	0.04 ± 0.52
Salinity	0.005 ± 0.029	0.004 ± 0.029	0.001 ± 0.024	0.000 ± 0.031	0.016 ± 0.025
Oxygen	21.8 ± 8.3	1.7 ± 7.2	20.1 ± 8.3	-13.6 ± 13.0	18.6 ± 10.7
O2 % sat	7.5%	0.5%	7.0%	-4.6%	6.5%
AOU	-21.4 ± 6.4	-1.6 ± 5.8	-19.8 ± 6.4	12.9 ± 11.5	-18.1 ± 8.4

Table 2 Differences. The standard deviations are the larger of the two years in Table 1 that are being compared.

WORKS CITED

Anderson, L.A., Sarmiento, J.L., 1994. Redfield ratios of remineralization determined by nutrient data analysis. Global Biogeochem. Cycles 8, 65–80. https://doi.org/10.1029/93GB03318

Blanchette, C.A., Wieters, E.A., Broitman, B.R., Kinlan, B.P., Schiel, D.R., 2009. Trophic structure and diversity in rocky intertidal upwelling ecosystems: A comparison of community patterns across California, Chile, South Africa and New Zealand. Prog. Oceanogr. 83, 107–116. https://doi.org/10.1016/j.pocean.2009.07.038

Brewer, P.G., Peltzer, E.T., 2017. Depth perception: the need to report ocean biogeochemical rates as functions of temperature, not depth. Philos. Trans. A. Math. Phys. Eng. Sci. 375. https://doi.org/10.1098/rsta.2016.0319

Bullister, J.L., 2015. Atmospheric Histories (1765-2015) for CFC-11, CFC-12, CFC-113, CCl4, SF6 and N20 (NCEI Accession 0164584). https://doi.org/10.3334/CDIAC/otg.CFC_ATM_Hist_2015

Bullister, J.L., Fine, R.A., Smethie, W.M.J., Warner, M.J., Weiss, R.F., 2000. Global Integration and Interpretation of WOCE CFC data. 2000 U.S. WOCE Report, U.S. WOCE Implementation Report Number 12.

Bullister, J.L., Wisegarver, D.P., Menzia, F.A., 2002. The solubility of sulfur hexafluoride in water and seawater. Deep. Res. Part I Oceanogr. Res. Pap. 49, 175–187. https://doi.org/10.1016/S0967-0637(01)00051-6

Capotondi, A., Alexander, M.A., Bond, N.A., Curchitser, E.N., Scott, J.D., 2012. Enhanced upper ocean stratification with climate change in the CMIP3 models. J. Geophys. Res. Ocean. 117. https://doi.org/10.1029/2011JC007409

Cha, S.C., Moon, J.H., Song, Y.T., 2018. A recent shift toward an El Niño-like ocean state in the Tropical Pacific and the resumption of ocean warming. Geophys. Res. Lett. 45, 11,885-11,894. https://doi.org/10.1029/2018GL080651

Czeschel, R., Stramma, L., Johnson, G.C., 2012. Oxygen decreases and variability in the eastern equatorial Pacific. J. Geophys. Res. Ocean. 117. https://doi.org/10.1029/2012JC008043

Czeschel, R., Stramma, L., Weller, R.A., Fischer, T., 2015. Circulation, eddies, oxygen, and nutrient changes in the eastern tropical South Pacific Ocean. Ocean Sci 11, 455–470. https://doi.org/10.5194/os-11-455-2015

Deutsch, C., Berelson, W., Thunell, R., Weber, T., Tems, C., McManus, J., Crusius, J., Ito, T., Baumgartner, T., Ferreira, V., Mey, J., Van Geen, A., 2014. Centennial changes in North Pacific anoxia linked to tropical trade winds. Science (80-.). 345, 665–668. https://doi.org/10.1126/science.1252332

Doney, S.C., Bullister, J.L., 1992. A chlorofluorocarbon section in the eastern North Atlantic. Deep Sea Res. Part A, Oceanogr. Res. Pap. 39, 1857–1883. https://doi.org/10.1016/0198-0149(92)90003-C

Fine, R.A., 2011. Observations of CFCs and SF6 as ocean tracers. Ann. Rev. Mar. Sci. 3, 173–95. https://doi.org/10.1146/annurev.marine.010908.163933

Fine, R.A., Maillet, K.A., Sullivan, K.F., Willey, D., 2001. Circulation and ventilation flux of the Pacific Ocean. J. Geophys. Res. Ocean. 106, 22159–22178. https://doi.org/10.1029/1999jc000184

Fine, R.A., Peacock, S., Maltrud, M.E., Bryan, F.O., 2017. A new look at ocean ventilation time scales and their uncertainties. J. Geophys. Res. Ocean. 122, 3771–3798. https://doi.org/10.1002/2016JC012529

Fine, R.A., Peterson, W.H., Ostlund, H.G., 1987. The penetration of tritium into the Tropical Pacific. J. Phys. Oceanogr. 17, 553–564. https://doi.org/10.1175/1520-0485(1987)017<0553:tpotit>2.0.co;2

Gnanadesikan, A., Russell, J.L., Zeng, F., 2007. How does ocean ventilation change under global warming? Ocean Sci. 3, 43–53. https://doi.org/10.5194/os-3-43-2007

Gruber, N., Gloor, M., Fan, S.M., Sarmiento, J.L., 2001. Air-sea flux of oxygen estimated from bulk data: Implications for the marine and atmospheric oxygen cycles. Global Biogeochem. Cycles 15, 783–803. https://doi.org/10.1029/2000GB001302

Ito, T., Minobe, S., Long, M.C., Deutsch, C., 2017. Upper ocean O2 trends: 1958–2015. Geophys. Res. Lett. 44, 4214–4223. https://doi.org/10.1002/2017GL073613

Jenkins, W.J., 1982. Oxygen utilization rates in North Atlantic subtropical gyre and primary production in oligotrophic systems. Nature 300, 246–248. https://doi.org/10.1038/300246a0

Jenkins, W.J., 1977. Tritium-helium dating in the sargasso sea: A measurement of oxygen utilization rates. Science (80-.). 196, 291–292. https://doi.org/10.1126/science.196.4287.291

Karstensen, J., Stramma, L., Visbeck, M., 2008. Oxygen minimum zones in the eastern tropical Atlantic and Pacific oceans. Prog. Oceanogr. 77, 331–350. https://doi.org/10.1016/j.pocean.2007.05.009

Keeling, R.E., Körtzinger, A., Gruber, N., 2010. Ocean deoxygenation in a warming world. Ann. Rev. Mar. Sci. 2, 199–229. https://doi.org/10.1146/annurev.marine.010908.163855

Keeling, R.F., Garcia, H.E., 2002. The change in oceanic O2 inventory associated with recent global warming. Proc. Natl. Acad. Sci. U. S. A. 99, 7848–7853. https://doi.org/10.1073/pnas.122154899

Llanillo, P.J., Pelegrí, J.L., Talley, L.D., Peña-Izquierdo, J., Cordero, R.R., 2018. Oxygen pathways and budget for the Eastern South Pacific Oxygen Minimum Zone. J. Geophys. Res. Ocean. 123, 1722–1744. https://doi.org/10.1002/2017JC013509

Lukas, R., 1986. The termination of the Equatorial Undercurrent in the eastern Pacific. Prog. Oceanogr. https://doi.org/10.1016/0079-6611(86)90007-8

Luyten, J.R., Pedlosky, J., Stommel, H., 1983. The ventilated thermocline. J. Phys. Oceanogr. 13, 292–309. https://doi.org/10.1175/1520-0485(1983)013<0292:tvt>2.0.co;2

McGregor, S., Timmermann, A., Stuecker, M.F., England, M.H., Merrifield, M., Jin, F.F., Chikamoto, Y., 2014. Recent walker circulation strengthening and pacific cooling amplified by atlantic warming. Nat. Clim. Chang. 4, 888–892. https://doi.org/10.1038/nclimate2330

Mecking, S., Langdon, C., Feely, R.A., Sabine, C.L., Deutsch, C.A., Min, D.H., 2008. Climate variability in the North Pacific thermocline diagnosed from oxygen measurements: An update based on the U.S. CLIVAR/CO2 Repeat Hydrography cruises. Global Biogeochem. Cycles 22. https://doi.org/10.1029/2007GB003101

Mecking, S., Warner, M.J., Bullister, J.L., 2006. Temporal changes in pCFC-12 ages and AOU along two hydrographic sections in the eastern subtropical North Pacific. Deep. Res. I 53, 169–187.

Merrifield, M.A., 2011. A shift in western tropical Pacific sea level trends during the 1990s. J. Clim. 24, 4126–4138. https://doi.org/10.1175/2011JCLI3932.1

Merrifield, M.A., Maltrud, M.E., 2011. Regional sea level trends due to a Pacific trade wind intensification. Geophys. Res. Lett. 38. https://doi.org/10.1029/2011GL049576

Murray, C.N., Riley, J.P., 1969. The solubility of gases in distilled water and sea water—II. Oxygen. Deep Sea Res. Oceanogr. Abstr. 16, 311–320. https://doi.org/10.1016/0011-7471(69)90021-7

Olsen, A., Key, R.M., Van Heuven, S., Lauvset, S.K., Velo, A., Lin, X., Schirnick, C., Kozyr, A., Tanhua, T., Hoppema, M., Jutterström, S., Steinfeldt, R., Jeansson, E., Ishii, M., Pérez, F.F., Suzuki, T., 2016. The global ocean data analysis project version 2 (GLODAPv2) - An internally consistent data product for the world ocean. Earth Syst. Sci. Data 8, 297–323. https://doi.org/10.5194/essd-8-297-2016

Redfield, A.C., 1958. The biological control of chemical factors in the envrionment. Am. Sci. 46, 230. https://doi.org/10.2307/27827150

Redfield, A.C., 1934. On the proportions of organic derivations in sea water and their relation to the composition of plankton, James Johnstone Memorial volume. University Press of Liverpool, Liverpool, U.K.

Roemmich, D., Gilson, J., Davis, R., Sutton, P., Wijffels, S., Riser, S., 2007. Decadal spinup of the south pacific subtropical gyre. J. Phys. Oceanogr. 37, 162–173. https://doi.org/10.1175/JPO3004.1

Roemmich, D., Gilson, J., Sutton, P., Zilberman, N., 2016. Multidecadal change of the South Pacific Gyre circulation. J. Phys. Oceanogr. 46, 1871–1883. https://doi.org/10.1175/JPO-D-15-0237.1

Sarmiento, J.L., Gruber, N., 2006. Ocean Biogeochemical Dynamics. Princeton University Press.

Schmidtko, S., Stramma, L., Visbeck, M., 2017. Decline in global oceanic oxygen content during the past five decades. Nature 542, 335–339. https://doi.org/10.1038/nature21399

Sonnerup, Rolf E., Chang, B.X., Warner, M.J., Mordy, C.W., 2019. Timescales of ventilation and consumption of oxygen and fixed nitrogen in the eastern tropical South Pacific oxygen deficient zone from transient tracers. Deep. Res. Part I In Press.

Sonnerup, Rolf E, Chang, B.X., Warner, M.J., Mordy, C.W., 2019. Deep-Sea Research Part I Timescales of ventilation and consumption of oxygen and fixed nitrogen in the eastern tropical South Pacific oxygen deficient zone from transient tracers. Deep. Res. Part I 103080. https://doi.org/10.1016/j.dsr.2019.103080

Sonnerup, R.E., Mecking, S., Bullister, J.L., 2013. Transit time distributions and oxygen utilization rates in the Northeast Pacific Ocean from chlorofluorocarbons and sulfur hexafluoride. Deep. Res. Part I Oceanogr. Res. Pap. 72, 61–71. https://doi.org/10.1016/j.dsr.2012.10.013

Sonnerup, R.E., Mecking, S., Bullister, J.L., Warner, M.J., 2015. Transit time distributions and oxygen utilization rates from chlorofluorocarbons and sulfur hexafluoride in the Southeast Pacific Ocean. J. Geophys. Res. Ocean. 120, 3761–3776. https://doi.org/10.1002/2015JC010781

Sonnerup, R.E., Quay, P.D., Bullister, J.L., 1999. Thermocline ventilation and oxygen utilization rates in the subtropical North Pacific based on CFC distributions during WOCE. Deep. Res. Part I Oceanogr. Res. Pap. 46, 777–805. https://doi.org/10.1016/S0967-0637(98)00092-2

Stramma, L., Johnson, G.C., Firing, E., Schmidtko, S., 2010. Eastern Pacific oxygen minimum zones: Supply paths and multidecadal changes. J. Geophys. Res. Ocean. 115. https://doi.org/10.1029/2009JC005976

Stramma, L., Johnson, G.C., Sprintall, J., Mohrholz, V., 2008. Expanding oxygen-minimum zones in the tropical oceans. Science (80-.). 320, 655–658. https://doi.org/10.1126/science.1153847

Thiele, G., Sarmiento, J.L., 1990. Tracer dating and ocean ventilation. J. Geophys. Res. 95, 9377. https://doi.org/10.1029/jc095ic06p09377

Vecchi, G.A., Soden, B.J., Wittenberg, A.T., Held, I.M., Leetmaa, A., Harrison, M.J., 2006. Weakening of tropical Pacific atmospheric circulation due to anthropogenic forcing. Nature 441, 73–76. https://doi.org/10.1038/nature04744

Wanninkhof, R., Ledwell, J.P., Watson, A.J., 1991. Analysis of sulfur hexafiuoride in seawater, Journal of Geophysical Research. https://doi.org/10.1029/91JC00104

Warner, M.J., Weiss, R.F., 1985. Solubilities of chlorofluorocarbons 11 and 12 in water and seawater. Deep Sea Res. Part A, Oceanogr. Res. Pap. 32, 1485–1497. https://doi.org/10.1016/0198-0149(85)90099-8

Waugh, D.W., Primeau, F., DeVries, T., Holzer, M., 2013. Recent changes in the ventilation of the Southern Oceans. Science (80). 568.

Weiss, R.F., 1970. The solubility of nitrogen, oxygen and argon in water and seawater. Deep. Res. Oceanogr. Abstr. 17, 721–735. https://doi.org/10.1016/0011-7471(70)90037-9

Wolberg, J.R., 1967. Prediction Analysis. D. Van Nostrand Company, Inc.

Wyrtki, K., 1974. Equatorial Currents in the Pacific 1950 to 1970 and Their Relations to the Trade Winds. J. Phys. Oceanogr. 4, 372–380. https://doi.org/10.1175/1520-0485(1974)004<0372:ecitpt>2.0.co;2